JBC Papers in Press. Published on July 25, 2014 as Manuscript M114.580688
The latest version is at http://www.jbc.org/cgi/doi/10.1074/jbc.M114.580688

Multifunctional Roles for the Protein Translocation Machinery in RNA Anchoring to the Endoplasmic Reticulum*

Sujatha Jagannathan[1,†], Jack C.-C. Hsu[2,†], David W. Reid[2], Qiang Chen[1], Will J. Thompson[3], Arthur M. Moseley[3], and Christopher V. Nicchitta[1,2*]

[1,2]From the Departments of Cell Biology[1], Biochemistry[2], and the Duke Proteomics Core Facility[3]
Duke University Medical Center, Durham, NC 27710 USA

[†] These authors contributed equally to this study.

*Running title: *Mechanisms of mRNA anchoring to the endoplasmic reticulum*

*To whom correspondence should be addressed: Christopher V. Nicchitta, PhD, Department of Cell Biology, Box 3709, Duke University Medical Center, Durham, NC 27710 USA Tel: (919) 684-8948; Fax: (919) 684-5481; Email: christopher.nicchitta@duke.edu

Keywords: endoplasmic reticulum (ER), RNA-protein interaction, RNA localization, ribosome, signal recognition particle, protein translocation

Background: ER-localized mRNAs are anchored to the ER via their functional engagement with translocon-bound ribosomes.
Results: Ribosome-engaged mRNAs are ER-bound through distinct and mRNA-selective mechanisms.
Conclusion: Multiple ER membrane proteins, including the Sec61 complex, display RNA binding activity and anchor select mRNAs to the ER.
Significance: These data reveal new functions for the translocation machinery and advance understanding of RNA localization to the ER.

ABSTRACT:

mRNAs encoding cytosolic and signal sequence-bearing proteins are translated by free and endoplasmic reticulum (ER)-bound ribosomes, respectively. Recent ribosome footprinting studies have also demonstrated translation of cytosolic protein-encoding mRNAs on ER-bound ribosomes, findings that raise important questions regarding the mechanism of ribosome and mRNA localization and association with the ER. Using a semi-intact HeLa cell model, we performed a polysome solubilization screen and identified conditions that biochemically distinguish polysomes engaged in the translation of distinct cohorts of mRNAs. RNA-protein UV photocrosslinking studies revealed numerous ER integral membrane proteins with RNA binding activity, consistent with direct RNA anchoring functions. Quantitative proteomic analyses of HeLa cytosolic and two classes of ER-bound polysomes identified translocon components as selective polysome-interacting proteins. Notably, the Sec61 complex was highly enriched in polysomes engaged in the translation of endomembrane organelle proteins whereas whereas translocon accessory proteins such as ribophorin I were present in all subpopulations of ER-associated polysomes. Analyses of the protein composition of oligo(dT)-selected UV photocrosslinked protein-RNA adducts identified Sec61α,β and ribophorin I, suggesting roles for the protein translocation and modification machinery in mRNA anchoring to the ER. We propose that multiple mechanisms of mRNA and ribosome association with ER operate to enable a transcriptome-wide function for the ER in cellular protein synthesis.

All eukaryotic cells localize secretory and membrane protein-encoding mRNAs to the endoplasmic reticulum (ER), the entry portal to the secretory pathway (1-3). ER-directed RNA localization operates on a remarkably large scale, where up to 50% of the genome encoding topogenic signal-bearing proteins (4), and by a mechanism quite distinct from that established for more prominent examples of RNA localization (5,6). In the majority of these latter cases, RNA localization occurs via motor protein-based transport of translationally-repressed, "zip code" element-encoding mRNAs to the cell periphery (5,6). RNA localization to the ER, in contrast, utilizes a co-translational mechanism, the signal recognition particle (SRP) pathway, does not require motor protein-based transport, and uses localization information encoded in the nascent protein rather than the mRNA (3,7,8).

Although SRP pathway function in RNA localization to the ER is well-established, recent investigations into the subcellular partitioning of mRNAs and their translation, as well as the biochemical basis of their ER association, have revealed an unexpected complexity in the ER-associated mRNA transcriptome (9-12). Notably, the near entirety of the mRNA transcriptome (including cytosolic and nucleoplasmic-encoding mRNAs) undergoes translation on ER-bound ribosomes and ER-associated mRNAs differ in their requirement for ribosome engagement as the primary mechanism of their ER association (12-15). By the latter criterion, one class of mRNAs has distinguished itself - the mRNAs encoding resident proteins of the endomembrane organelles. This mRNA cohort shares a number of molecular characteristics including translation- and signal peptide-independent ER localization, ribosome-independent anchoring to the ER, and a uniquely high ER enrichment (12,13,15). Importantly, these findings are not unique to mammalian cells; translation-independent localization of mRNAs to the yeast ER as well as the E. coli inner membrane has also been reported (16-18).

At present, little is known regarding the *in vivo* mechanisms of mRNA localization and anchoring to the ER (11,19). Presumably, direct mRNA anchoring to the ER membrane would require RNA binding proteins (RBPs), which are known to serve diverse functions in RNA localization, translational regulation and stability (20,21). Indeed, recent studies have identified ribosome receptor RRBP1 (p180), a coiled-coil multi-domain ER resident membrane protein, as a general ER poly(A) mRNA anchoring protein (14,22). p180 is multifunctional; as a microtubule binding protein, it participates in the dynamic regulation of ER distribution in the cell, it has been shown to enhance ribosome loading onto selected mRNAs, and to regulate the stability of ER-associated mRNAs (23-27). p180 is reported to bind mRNAs non-specifically, however, and so the question of how mRNAs undergo selective association with the ER membrane remains largely unanswered.

Here we used biochemical, genomic, optical imaging, and proteomic approaches to investigate mechanisms of mRNA-ER interaction in mammalian cells. These studies reveal a diversity of RNA anchoring processes where cytosolic- and secretory protein-encoding mRNAs display similar anchoring mechanisms and RNA binding protein compositions, and which are distinct from those utilized by endomembrane protein-encoding mRNAs. Intriguingly, proteomic analysis of native and photocrosslinked ER-bound mRNAs identified components of the protein translocation machinery as ER-mRNA anchoring proteins and suggests multifunctional roles for these proteins in the selective localization and anchoring of mRNAs to the ER.

Experimental Procedures:

Cell culture and sequential detergent fractionation. HeLa cells were maintained at 37ºC, 5% CO_2 in Dulbecco's modified Eagle's medium (DMEM; Mediatech) supplemented with 10% fetal bovine serum (FBS; Gibco). For detergent fractionations, cell cultures (75-90% confluence) were incubated on ice for 20min in PBS/$MgCl_2$, 50μg/ml cycloheximide (CHX) (Sigma), to depolymerize the microtubule network (4^{o}C) and stabilize polyribosomes (CHX). Cytosol fractions were obtained by treating cell monolayers with a plasma membrane permeabilization buffer (110mM KCl, 25mM K-HEPES at pH 7.4, 1mM $MgCl_2$, 0.015% digitonin (Calbiochem), 0.1mM EGTA, 40U/ml RNAseOUT (Invitrogen), 1mM DTT). The cytosol fraction was recovered, the cells rinsed in a buffer of identical composition containing 0.004% digitonin, and the two fractions

combined. Subfractionation of the endoplasmic reticulum was performed by first treating the digitonin-extracted cell cultures with the indicated detergents at 10-fold critical micelle concentration, in a buffer consisting of 500mM Tris-HCl, pH 7.0, 1mM $MgCl_2$, 40U/ml RNAseOUT and 2mM DTT, and subsequently extracting the cells in 2% dodecylmaltoside (DDM), 200mM KCl, 25mM K-HEPES at pH 7.4, 10mM $MgCl_2$, 40 U/ml RNAseOUT and 2 mM DTT (28-30).

Polyribosome profiling and negative staining electron microscopy. Polyribosomes from the different subcellular fractions, prepared as described above, were resolved on 15-50% sucrose gradients and fractioned using a Teledyne/Isco gradient fractionator, as described previously (29,30). To assess polysome translation status, cell cultures were supplemented with 150µCi/ml of [^{35}S]Met/Cys for 10 min in the presence or absence of cycloheximide, fractionated as above, and fractions resolved by sucrose gradient centrifugation. Radiolabeled proteins were recovered by trichloroacetic acid (TCA) (10% v:v) precipitation onto filter paper squares, boiled in 10% TCA, rinsed in cold 10% TCA, acetone-extracted, dried, and radioactivity measured by scintillation counting. Negative staining electron microscopy of the various polysome fractions was performed as described in (31).

RNA extraction and quantitative RT-PCR. Total Samples were supplemented with Alien RNA (Life Techologies) and total RNA extracted by acid guanidinium thiocyanate-phenol-chloroform extraction (32). Cell-equivalent quantities of total RNA were used to prepare cDNA using M-MLV reverse transcriptase (Promega) and random hexamer primers (Roche). Quantitative RT-PCR was performed on a 7900HT Sequence Detection System (Applied Biosystems) using Power SYBR® green PCR mastermix (Applied Biosystems) and the following primers:

GRP94:
F: CTGGAAATGAGGAACTAACAGTCA;
R: TCTTCTCTGGTCATTCCTACACC
HSPA5 (BiP):
F: CAACCAACTGTTACAATCAAGGTC;
R: CAAAGGTGACTTCAATCTGTGG
CALR:
F: CGCTGCCGGAGGGTCGTTTT;
R: GGGAAGTCCACCCGTCTCCGT,
B2M:
F: TTCTGGCCTGGAGGCTATC;
R: TCAGGAAATTTGACTTTCCATTC
THPO:
F: TGCTGTGGACTTTAGCTTGG;
R: CTGCTCCCAGAATGTCCTGT
VEGFA:
F: CCTTGCTGCTCTACCTCCAC;
R: CCACTTCGTGATGATTCTGC
18S rRNA:
F: CACGGGAAACCTCACCCGGC;
R: CGGGTGGCTGAACGCCACTT.

The data were analyzed by the ddCt method using the Alien RNA as a normalizer. Except for 18S rRNA, all primers were designed to be intron-spanning using the Primer3-based ProbeFinder software (Roche).

Oligonucleotide microarray and data analysis RNA integrity was was first determined with the Agilent Bioanalyzer (Agilent Technologies); all samples analyzed had RIN values > 9. Total RNA was processed for oligonucleotide microarray analysis using a Whole Transcriptome amplification kit (Agilent Technologies) and cDNAs were hybridized to GeneChip Human Gene 1.0 ST Arrays (Affymetrix). Microarray data were processed using the Genomics Suite™ software (Partek Inc.) package and log_2-transformed intensity values exported after background correction by GC-RMA, probe summarization by Tukey's biweight median method, and no normalization. The minimum intensity cut-off value was set at the lower quartile of the dataset and the intensity values for genes represented by multiple probe sets were averaged.

Gene categorization. Genes were categorized into cytosolic/nuclear (cytosolic, nucleoplasmic and mitochondrial proteins), endomembrane-resident (ER, lysosome, Golgi, endosomal or nuclear envelope membrane-resident) or secretory pathway cargo (secretory and membrane proteins) based on the subcellular location GO categories assigned by Uniprot. The assignments were then manually verified using the following sequence features: signal peptide (predicted by SignalP), transmembrane domain (predicted by TMHMM) and mitochondrial transit peptide (predicted using TargetP) and entries with ambiguous assignments were removed from further analyses. Membrane proteins with a C-terminal anchor were removed from both endomembrane resident and cargo

categories since their targeting to the ER is post-translational.

Protein, mRNA, lipid imaging. Immunoblot analyses were performed as previously described (28-30). Single molecule mRNA imaging was performed with Stellaris FISH probes (Cell Search Technologies) as per manufacturer's protocols. ER membrane integrity was imaged with ER tracker blue-white DPX (Invitrogen). Ceramide imaging was performed using BODIPY FL C5-ceramide (Invitrogen), as per manufacturer's instructions.

Fluorescence imaging and analysis. All imaging was performed on a Deltavision Elite deconvolution microscope (Applied Precision) equipped with 100x NA 1.4 oil immersion objective (UPlanSApo 100XO; Olympus) and a high-resolution CCD camera (CoolSNAP HQ2; Photometrics). Images were acquired as Z-stacks at 0.2μm intervals, at identical exposure settings across all samples for a given imaged protein, RNA, or lipid. Image data were deconvolved using the SoftWoRx program (Applied Precision) and processed on ImageJ/FIJI and Adobe Photoshop (Adobe Systems) to render maximum intensity projections, merge channels and pseudocolor images. Adjustments in image brightness/contrast were limited to linear changes and were applied uniformly across all images in a given experiment. The number of RNA molecules per cell was measured using the spot-counting module of the Imaris 7.3 software (Bitplane) with automated thresholding. The mean number of RNA spots/cell was calculated for 10-45 cells in each sample and plotted using GraphPad Prism, with error bars representing standard error of mean. The final figures were assembled on Adobe Illustrator v. 15.1.0 (Adobe Systems).

RNA Crosslinking to Endoplasmic Reticulum Membrane Proteins. Canine rough microsomes (RM) were irradiated with 264nm UV light (Stratagene Stratalinker) for 30 min on ice, nuclease digested and the RNA [^{32}P]-labeled, as per below, following purification of the membrane protein fraction by either alkali extraction or Triton X-114 cloud point partitioning (33,34).

RNA-dependent T4 RNA Ligase Labeling of UV-Irradiated RM. RM-associated RNAs were digested with mung bean nuclease at a final concentration of 1U/μg RNA and incubated at 30^{o}C for 1 hr. RM were collected by ultracentrifugation and the RM pellet resuspended in lysis buffer. For T4 RNA ligase reaction, the RM fractions were adjusted to a final concentration of 50 mM Tris-HCl, pH 7.5, 10mM $MgCl_2$, 1mM DTT, 15% DMSO, 1mM ATP, 80 μCi [5'-^{32}P] cytidine 3',5'-bis(phosphate),1 U/μl T4 RNA ligase (New England Biolabs) and incubation at 4^{o}C. The lysate was collected, TCA precipitated, and analyzed by SDS-PAGE and phosphorimaging.

Proteomic analysis of HeLa polysomes. HeLa cell cultures were fractionated as described above and polyribosomes from the cytosol, Brij-sensitive ER, and Brij-resistant ER fractions were purified by sucrose density gradient centrifugation. The polyribosome fractions were concentrated by ultracentrifugation and 30 μg of each sample was concentration-normalized to approximately 0.1 μg/μL with 50 mM ammonium bicarbonate (AmBic), and then supplemented with Rapigest SF surfactant (Waters) to a final concentration of 0.1% w/v. Cysteine reduction (10 mM DTT), alkylation (20mM iodoacetamide) and trypsin digestion was then performed. After digestion, all samples were spiked with 33 fmol ADH1_YEAST digest (Massprep standard, Waters Corporation) per microgram total protein as a surrogate standard, acidified to 1% TFA and heated to 60^{o}C for 2 hours to hydrolyze Rapigest surfactant. Finally, the samples were taken to dryness in a SpeedVac (Eppendorf) and resuspended in 100 mM ammonium formate (pH 10) at a concentration of 1.0 ug/uL prior to analysis.

Quantitative two-dimensional liquid chromatography – tandem mass spectrometry (LC/LC-MS/MS) was performed on 3 μg of protein digest per sample, and each sample was analyzed twice, once in ion-mobility MS mode (HDMS^{E}) for simultaneous qualitative/quantitative analysis, and once by data-dependent acquisition (DDA) mode for supplementary peptide identifications (35-37). Following all analyses, data was imported into Rosetta Elucidator v3.3 (Rosetta Biosoftware, Inc), and all LC/LC-MS runs were aligned based on the accurate mass and retention time of detected ions ("features") using the PeakTeller algorithm (Elucidator). The peptide abundance was calculated based on area-under-the-curve (AUC) of aligned features across all runs. The MS/MS data was searched against a SwissProt database with human taxonomy, which

also contained a reversed-sequence "decoy" database for false positive rate determination. Database searching for $HDMS^E$ data was performed in PLGS v2.5, and for DDA data using Mascot v2.2. Database searches were combined within the Elucidator software package and aggregate scoring was performed using the PeptideProphet algorithm. The data was annotated at a PeptideProphet score of 0.73, resulting in a 0.7% peptide false discovery rate (38,39). To allow relative mol composition comparisons for the different components making up the polyribosome fractions, we used the "Best Flier" method of Silva et al. with minor modifications as previously described (40-42).

Proteomic analysis of canine rough microsome-associated mRNPs. Canine pancreas rough microsomes were detergent solubilized and the polysome fraction obtained by sucrose gradient velocity sedimentation. Polysome fractions were pooled and concentrated by ultracentrifugation. Polysome pellets were then gently resuspended and a binding control fraction prepared by digestion of one half of the sample with staphylococcal nuclease. Following addition of 15 mm EDTA to all samples, to dissociate the ribosomal subunits and release mRNPs, poly(A) mRNPs were selected on oligo-dT7 resin (GE Healthcare). Following extensive washing in EDTA-supplemented buffers, poly(A)mRNA-associated proteins were released by addition of 10 mM AmBic, 15% dimthylformamide. Eluted proteins were concentrated by TCA precipitation, separated on Bis/Tris gradient gels (Invitrogen), and in-gel digestion performed as described in (43). Approximately ½ of each digest (5 μL) was fractionated on a C18 column (Waters) using a gradient of 5 to 40% acetonitrile with 0.1% formic acid, on a nanoAcquity liquid chromatograph (Waters). Electrospray ionization was used to introduce the sample in real-time to a Q-Tof Synapt G1 mass spectrometer (Waters), collecting data for each sample in DDA mode. Raw data was processed in Mascot Distiller (v2.3) and searched in Mascot v2.2 (Matrix Science) against the NCBInr database with mammalian taxonomy. Scaffold (v3.6.2, Proteome Software Inc.) was used to validate MS/MS based peptide and protein identifications. Measured peptide and protein level false-discovery rate (FDR) were both determined to be 0.0% using the target-decoy strategy.

For photocrosslinking studies, RM were UV irradiated in a Stratalinker 24000 at 0.8 J/cm^2 for four cycles on ice. Samples were adjusted to a final concentration of 0.5M KOAc, 15 mM EDTA, 50U/ml RNaseOUT, protease inhibitor cocktail and incubated for 30 min on ice. KOAc/EDTA-washed RM were collected by ultracentrifugation and resuspended in a oligo(dT) resin equilibrium buffer (0.5% LiDS, 0.5M LiCl, 10mM Tris-HCl, pH 7.2, 5 mM DTT, 15 mM EDTA), heated to 65°C for 5 min and cooled on ice. The solubilized RM suspension was then centrifuged, to remove detergent-insoluble materials and the supernatant was chromatographed on oligo-dT7 resin (GE Healthcare). Unbound material was removed by extensive washing in oligo(dT) resin equilibrium buffer and the RNA-associated RBPs subsequently eluted by addition of a buffer consisting of 10 mM Tris-HCl, pH 7.2, 1 mM EDTA, 0.1 % Triton X-110 with 1:50 (v/v) RNase A/T1 Mix (Thermo Scientific) at RT for 30 min. Eluted proteins were concentrated by TCA precipitation and their composition assessed by immunoblot.

Results:

Divergent modes of ribosome-mRNA association with the ER membrane. In cell-free translation/translocation systems, mRNAs are co-translationally localized to the ER and anchored indirectly, via ribosome binding to the protein-conducting channel (3,8,44). In contrast, analyses of in situ mRNA-ER interactions, conducted with rough microsomes (RM), have demonstrated that ER-associated mRNAs can be binned into two broad classes – those that are bound via ribosome-dependent (indirect) and those that undergo ribosome-independent (direct) ER-mRNA anchoring (Fig.1A) (13,15,45-47). These differences are significant because they suggest that mRNA localization and anchoring to the ER is selective, regulated, and so may contribute significantly to gene expression.

To better understand mechanisms of ER-mRNA association, we developed methods to study mRNA-ER interactions in semi-intact cells, whose ER morphology and function more closely approximate the in vivo scenario and where cytosolic and ER-associated mRNAs can be reliably separated (48). Our experimental approach is schematically illustrated in Fig. 1A. First, tissue culture cells are permeabilized with a digitonin-

supplemented cytosol buffer to permeabilize the plasma membrane and release the cytoplasmic mRNA pool (28,49). The digitonin-permeabilized (semi-intact) cells are then treated with salts, chelating agents and/or detergents and mRNA-ER interactions assessed by examining the mRNA composition of the released and ER-associated fractions (13,15,45-47). Using HeLa cells as a model, we first examined the ER association properties of two mRNAs - β2-microglobulin (B2M), a secretory protein, and GRP94, a resident protein of the ER lumen, as previous studies with RM had identified these mRNAs as undergoing either ribosome-dependent (B2M) or ribosome-independent (GRP94) membrane association (13,15). In contrast to prior findings with RM, in semi-intact HeLa cells B2M transcripts remained wholly membrane-bound under conditions (high salt extraction) that yielded their efficient release from RM (Fig. 1B). The reason for these differences is not yet known, though it has been suggested that differences in endogenous nuclease activity, tissue source, and buffer composition used during RM isolation can significantly influence the biochemical properties of RM-associated mRNAs (46,50,51).

Because ER morphology and polysome structure in semi-intact cells more closely approximates the in vivo scenario then that of RM, where polysome structure is frequently compromised, we postulated that mRNA-ER interactions in semi-intact cells would be more stable to biochemical extraction. We thus screened detergent/salt admixtures for their ability to solubilize mRNAs from digitonin-permeabilized HeLa cells. Intriguingly, we found that extraction with Brij35/Tris or Brij58/Tris detergent/salt admixtures revealed divergent membrane association properties for B2M and GRP94 mRNAs, where B2M mRNAs were efficiently solubilized and GRP94 mRNAs were refractory to solubilization (Fig.1B). By varying the detergent component in the screen, we found that selective mRNA release correlated with detergent hydrophile-lipophile balance (HLB), with high HLB detergents, e.g., Brij35 (HLB = 17.0), yielding selective mRNA release and low HLB detergents such as Triton X-100 (HLB = 13.6) or the bile salt derivative CHAPSO efficiently solubilizing both B2M and GRP94 mRNAs. Importantly, the combination of high salt (0.5M Tris) and Brij detergent was synergistic; neither 0.5M Tris nor Brij detergent alone was sufficient for selective mRNA release (Fig. 1B). These findings were not unique to the B2M- and GRP94-encoding mRNAs; mRNAs encoding the secretory proteins β2-microglobulin (B2M), vascular endothelial growth factor A (VEGFA) and thrombopoietin (THPO) were efficiently solubilized in Tris/Brij35 buffers whereas mRNAs encoding the ER resident proteins GRP94, BiP and calreticulin (CALR) were refractory to Tris/Brij35 solubilization (Fig. 1C), suggesting that mRNAs undergo cohort-specific binding interactions with the ER.

Although we assayed mRNA release in the salt/detergent screen above, the mRNAs are ER-bound as polysomes and so the divergent solubilization behaviors could simply arise from differences in nascent polypeptide chains (e.g., signal sequence functionality, interactions with the protein translocation machinery), differences in ribosome loading and/or open reading frame size, and/or mRNA-specific binding interactions with components of the ER membrane, any or all of which could alter binding interactions and/or avidity. However, by accepted criteria (mean length, hydrophobicity score), the signal peptides of the two cohorts of mRNAs were quite similar (Table 1). In addition, comparisons of open reading frame and overall transcript length did not distinguish the two; THPO (36 kDa), for example, is encoded by an 1805 bp mRNA whereas CALR (48 kDa) is encoded by a 1929 bp mRNA, yet the two mRNAs display divergent modes of membrane association (Table 1). To address possible differences in translation/ribosome loading, we examined the translational status of the polysomes recovered in the Brij-sensitive (BrS) and Brij-resistant (BrR) fractions. When analyzed by sucrose density gradient centrifugation, the polysome profiles of the two fractions were quite similar (Fig. 1D), a conclusion that we confirmed by examining the EDTA sensitivity of the ribosome profiles and by rotary shadowing electron microscopy imaging of the polysome fractions (Fig.1D,H,I) (52). In addition, both polysome pools were translationally active; analysis of gradient fractions obtained from [^{35}S]Met/Cys-labeled cells demonstrated a high degree of overlap in the ribosome and [^{35}S] nascent polypeptide chain profiles (Fig. 1E). These

findings were further validated in experiments where cycloheximide was added prior to the addition of radiolabeled amino acids. Under these conditions, [^{35}S] incorporation was reduced by > 95%, with the remaining fraction likely representing ribosome-associated [^{35}S]Met/Cys] aminoacyl tRNAs. Lastly, the B2M (ca. 350 bp) and GRP94 (ca. 2300 bp) mRNAs were enriched in the polysome fractions in the absence, but not the presence of EDTA (Fig. 1F,G). Combined, these data are consistent with the view that polysomes are bound to the ER by multiple mechanisms and suggest that for the endomembrane resident mRNAs, the mRNA itself contributes to the binding interactions. Of particular interest, prior studies have demonstrated that native ribosome-Sec61 interactions are quite salt resistant, with only partial disruption reported at salt concentrations as high as 1.2M (53). It would appear, then, that the polysomes recovered in the BrS fraction are either bound to sites other then Sec61 and/or are bound to Sec61 in a manner distinct from the salt-resistant Sec61 binding behavior of the BrR polysomes.

ER-Associated mRNAs Are Partitioned Between Detergent-Induced Sphingolipid-Rich and Spingolipid-Poor ER Membrane Domains. That ER-associated mRNAs displayed distinct Brij solubilization profiles was of interest, as Brij detergents are well known to display selective membrane solubilization behavior, where they efficiently solubilize glycerophospholipids but are ineffective in solubilizing sphingolipids and subsets of integral membrane proteins (54,55). Although these findings have been interpreted as evidence for membrane microdomains, in the context of this study we considered that Brij detergents could serve as useful biochemical tools for identifying candidate ribosome and/or mRNA interacting proteins in the BrS and BrR fractions.

As a means of validating this approach, we examined ER-associated mRNAs and ER membrane structure in HeLa cells fractionated by the three-detergent sequence noted above. In these experiments, mRNAs were individually imaged by single molecule RNA fluorescence *in situ* hybridization (smRNA-FISH)(56), and ER membrane components by ER selective membrane and protein reagents.

Representative micrographs depicting B2M and GRP94 mRNA distributions through the sequential detergent extraction protocol are shown in Fig.2A, with quantification data included as insets. Similar to the data reported in Fig.1B, extraction of digitonin-permeabilized HeLa cells with the Brij/Tris buffer resulted in the release of ca. 75% of ER-associated B2M mRNAs but only ca. 10% of GRP94 mRNAs. Following extraction with dodecylmaltoside (DDM), GRP94 mRNAs and the remaining small fraction of Brij35-resistant B2M mRNAs were released. These data demonstrate, by an orthogonal approach, mRNA-selective modes of polysome association with the ER.

To assess the effects of sequential detergent extraction on ER membrane structure, we first visualized the ER network with ER Tracker Blue-White DPX (Fig.2B). Here, the ER Tracker Blue-White DPX staining patterns of intact and digitonin-treated cells were nearly identical, although overall intensities were diminished following digitonin treatment. We attribute the decrease in fluorescence intensity to a partial redistribution of ER-bound probe into the detergent-supplemented buffers. Subsequent treatment with Tris/Brij35 resulted in the complete loss of ER Tracker Blue-White DPX staining, indicative of a loss of ER membrane integrity. This conclusion was further supported by immunostaining for the ER lumenal protein GRP94, which was distributed throughout the ER of unfractionated and digitonin-treated cells and absent following Tris/Brij35 extraction (Fig.2C). Given the lipid selectivity of Brij detergents, we also examined HeLa ER sphingolipid distributions in experiments where HeLa cells were biosynthetically labeled with BODIPY FL C5-ceramide and subsequently fractionated (Fig.2D). BODIPY FL C5-ceramide undergoes concentration-dependent excimer formation that serves as a convenient marker of subcellular (e.g. Golgi) ceramide enrichment (57,58). Following short (5-min) labeling periods, the ER displayed diffuse BODIPY-ceramide fluorescence (green) with a perinuclear Golgi enrichment (red) (57,58) (Fig.2B). This staining pattern was enhanced following digitonin treatment, and BODIPY-ceramide excimer clusters were prominent in the Golgi (Fig.2D). Following Tris/Brij35 extraction however, BODIPY-ceramide distributions were

dramatically altered, with Golgi structures no longer discernible and the BODIPY-ceramide present throughout the ER (green channel) and as numerous sphingolipid-dense clusters (red channel) (Fig.2D). Subsequent extraction with DDM yielded a near complete loss of BODIPY-ceramide staining. These data provide a clear illustration of the lipid selectivity of Brij35 extraction (54), and allowed us to determine if GRP94 mRNAs were enriched in the Brij-induced ceramide clusters. Co-localization studies were thus performed where GRP94 smRNA FISH was performed on BODIPY-ceramide labeled HeLa cells (Fig.2E). As depicted, GRP94 mRNAs were largely if not entirely resolved from the ceramide clusters, though retained in the ceramide-rich ER remaining after Brij extraction. Combined with the data presented in Fig. 1, these data support the view that divergent binding interactions contribute to the phenomenon of ER-mRNA interactions.

Divergent Modes of ER-mRNA Association Are Characteristic of the ER-mRNA Transcriptome. To determine if the differing modes of mRNA-ER interaction described above reflected an mRNA transcriptome-wide organization of mRNA anchoring to the ER, we next determined the mRNA compositions of the BrS and BrR fractions by oligonucleotide microarray (Fig.3, Table S1). A histogram depicting mRNA enrichment in the BrR fraction is shown in Fig.3A and, interestingly, details a tailed, non-normal distribution. By fitting a two-component mixture model to these data (Fig.3B) we identified a major population of mRNAs with a median BrR distribution of 0.38 and a second, smaller population of mRNAs with a highly significant enrichment in the BrR fraction (median = 0.65). The mRNA distribution data determined by oligonucleotide microarray revealed that endomembrane resident protein-encoding transcripts were highly enriched in the BrR fraction. We thus analyzed the dataset in a three-category model where ER-associated mRNAs were sorted as either cytosolic ($mRNA_{cyt}$), secretory pathway cargo ($mRNA_{cargo}$), or endomembrane resident ($mRNA_{endo}$). Histograms depicting the fractional BrR enrichment for each category were plotted as a function of normalized gene count (Fig.3C). $mRNA_{cyt}$ were the most numerous (n=6687) and displayed the lowest BrR enrichment values (median=0.32). $mRNA_{cargo}$ (n=2931) displayed a median BrR enrichment of 0.44 and $mRNA_{endo}$ (n=734), a median BrR enrichment of 0.59. These differences are further illustrated in a cumulative gene density plot (Fig.3D), where the qRT-PCR determined BrR partitioning values for the genes examined in Fig.1C are also indicated, and demonstrate both the divergent membrane association properties of the ER-associated transcripts as well as a strong correlation between the mRNA partitioning values determined by oligonucleotide microarray and qRT-PCR (solid circles). Statistical analysis of these data by the Kolmogorov-Smirnov (K-S) test indicated that the differences in the BrR distributions of the three gene categories were highly significant ($p < 10^{-16}$; Table 2).

In further analyses, organelle-specific subcategories of $mRNA_{endo}$ were defined and their cumulative density distributions in the BrR fraction plotted (Fig.3E). Unexpectedly, an organelle-specific grouping revealed that mRNAs encoding lysosomal resident proteins were remarkably BrR-enriched and distinct from the ER- and Golgi-resident protein mRNAs, perhaps suggestive of a function for the ER in 'pre-lysosomal' biogenesis, as has been reported for pre-peroxisome biogenesis (59) (Fig.3E; Table S1). In the secretory pathway cargo cohort, we also compared the distribution of mRNAs encoding plasma membrane (Cargo-Mem) and secreted proteins (Cargo-Sec). Neither class of mRNAs deviated significantly from the total cargo population (Cargo), indicating that encoded topogenic signals (e.g., signal peptide, transmembrane domain) are not primary determinants of mRNA partitioning to the BrS or BrR fractions (Fig.3F). In addition, for those genes encoding signal sequences, there was no correlation between the calculated signal peptide hydrophobicity and mRNA enrichment in the BrR fraction (Fig.3G).

We also determined whether open reading frame length or ribosome loading, both of which could contribute to the avidity of mRNA/polysome association with the ER, correlated with mRNA partitioning to the BrR fraction. As shown in Figs.3H,I neither mRNA length nor ribosome loading density (number of ribosomes/mRNA) ((12)) correlated with the ER membrane association properties of the mRNA. In contrast, when mRNA enrichment in the BrR fraction was

plotted as a function of the fractional distribution to the ER (determined in (12), a strong correlation was observed (Fig.3J), i.e. mRNAs displaying the strongest localization to the ER also display the highest anchoring to the BrR-ER and vice versa. These data highlight the distinctive molecular signature of the endomembrane resident protein-encoding mRNAs and raise the important question of their mechanism of association with the ER membrane (12,13,15).

Identification of RNA-Binding ER Membrane Proteins. Past and recent studies have provided evidence for the direct (ribosome-independent) association of endomembrane mRNAs to the ER (10,12-16). Given the detergent solubilization properties of the endomembrane mRNAs reported above, we considered that this mRNA cohort might directly bind to resident integral membrane RNA binding proteins (RBPs), though it is equally plausible that mRNA anchoring could occur via binding interactions between soluble RBPs and cognate ER RBP binding proteins. To date, no resident ER integral membrane proteins containing canonical RNA binding domains have been identified. Recent proteomic screens have revealed, however, a surprising diversity of proteins with RNA binding activity, many of which lack known RNA binding domains and/or whose RNA binding activity remains to be characterized (60-63). Consistent with these findings, mRNA binding activity has been proposed for one resident ER membrane protein, p180 (RRBP1)(14).

As a relatively unbiased approach to the question of indirect or direct RNA anchoring to the ER, we screened for integral ER RNA binding proteins by UV-crosslinking, a 'zero-length' protein-nucleic acid crosslinking method (60,64). To focus the analysis on ER integral membrane proteins, experiments were performed with canine pancreas rough microsomes (RM), a highly enriched ER membrane preparation that is virtually devoid of other contaminating organelle membranes (65). The experimental protocol used is illustrated in Fig.4A. Here, RM were UV-irradiated to generate protein-RNA crosslinks, peripheral proteins released by salt/EDTA or mild alkali extraction (34), and the 'stripped' RM collected by ultracentrifugation. The irradiated, stripped RM were then digested with mung bean nuclease to generate protein-RNA adducts bearing free 3' OH groups, which were then selectively labeled using T4 RNA ligase/[^{32}P] cytidine 3'-5'bisphosphate (66). In contrast to alkaline extraction, which releases both peripheral and lumenal proteins, the salt/EDTA washed RM contain substantial quantities of lumenal proteins and so were subjected to multiple rounds of Triton X-114 partitioning to isolate the ER integral membrane protein fraction (33,67). Shown in Fig.4B are Coomassie Blue-stained SDS-PAGE gels of the two ER membrane protein fractions (alkali-extracted and TX-114 selected), where gels were loaded as either membrane equivalents, to illustrate the high relative abundance of ribosomal and lumenal vs. integral membrane proteins, or protein equivalents, to more clearly reveal the ER integral membrane protein proteome. Immunoblots for the lumenal proteins GRP94 and BiP and the membrane proteins ribophorin I, Sec61α and TRAPα demonstrate that the two procedures effectively separate soluble and integral membrane proteins (Fig.4C). Importantly, these data demonstrate that the integral membrane protein fractions (DP for the TX-114 extraction and P for the alkali extraction) lack "false positives"; the soluble proteins BiP and GRP94 were entirely absent from the integral membrane protein fractions.

The results of the [^{32}P] pCp/T4 RNA ligase labeling experiments are depicted in Fig.4D and demonstrate that the labeling reaction was strictly T4 RNA ligase-dependent (Fig.4D, lane 1 vs. lane 2) and yielded numerous radiolabeled protein-RNA adducts of apparent molecular weights ranging from 15 kDa to 70 kDa in the ER integral membrane protein fractions obtained via Triton X-114 partitioning (DP) or alkali-extraction (Alkali) (Fig.4D, lanes 3,4, respectively). These data demonstrate that numerous ER membrane proteins display direct RNA binding activity. Because this protocol for detecting RNA binding activity does not distinguish between mRNA, rRNA, tRNA, and/or non-translated RNAs, complementary approaches were developed to identify the ER membrane proteins functioning in mRNA anchoring (68-70).

Proteomic Analyses of Cytosolic and ER-Bound Polysomes Identifies Candidate ER-mRNA Anchoring Proteins. The molecular characteristics of the endomembrane protein-encoding mRNAs

described above and in past studies (12,13,15), suggested a number of strategies for the identification of l ER integral membrane RNA anchoring proteins and three such strategies were used here. In one approach, we determined the Brij solubilization properties of a panel of HeLa ER resident membrane proteins previously reported to function as ribosome-binding proteins and/or identified in a recent comprehensive 'mRNA-interactome' screen in HeLa cells, as a means to identify candidate RNA anchoring proteins in the BrR fraction (Fig.5A) (60). Intriguingly, the ER membrane proteins examined displayed highly divergent Brij solubilization profiles. For example, Ire1α, an unfolded protein sensor and mRNA endonuclease (71), SRα, the SRP-interacting subunit of the SRP receptor (72), and reticulons 4b and 4c, which confer tubular ER membrane structure (73,74), were highly enriched in the BrS fraction. SRα and reticulon 4a, the high molecular weight isoform of reticulons 4b and 4c, were recently identified as members of the HeLa mRNA interactome (Castello et al, 2012), and thus might contribute to mRNA-ER interactions in the BrS, but not BrR, fractions. The ribosome receptor p180 (RRBP1) was detected as two isoforms: a 180kDa form (p180) with reported ribosome receptor and microtubule binding activity (25,75) and more recently as a candidate general ER poly(A)-mRNA binding protein (14); and a 130 kDa form (ES130) which lacks the ribosome-binding decapeptide repeat motif but retains the coiled-coil microtubule binding domain (76). The two isoforms encode a common transmembrane domain yet their Brij35 solubilization profiles were strikingly different, with ES130 partitioning to the BrS ER and p180 to the BrR ER. Both isoforms contain the lysine-rich domain recently proposed to function in mRNA binding, which, although consistent with a role in general poly(A) mRNA anchoring to the ER, would be inconsistent with a selective endomembrane mRNA anchoring function. p180/ES130 was not, however, identified as either a validated or candidate RBP in the HeLa mRNA interactome (60). Consistent with these findings, shRNA-mediated stable knockdown of p180/ES130 in HeLa cells did not alter ER-associated calreticulin mRNA levels, though a small shift in calreticulin mRNA partitioning between the BrS- and BrR-ER membrane domains was observed (data not shown). The lack of a discernible effect of p180 knockdown on ER-mRNA binding may reflect redundancies in anchoring mechanisms and/or cell type-specific functions of p180 and is under further study.

Ribophorin I (RPN1), a subunit of the oligosaccharyltransferase complex, and TRAPα (SSR1) reside in close physical proximity to ER-bound ribosomes (77-79). Ribophorin I was recently identified as a HeLa RBP and TRAPα a candidate HeLa RBP; both proteins were distributed between the BrS and BrR fractions, enriched in the BrR fraction, and so were scored as candidate ER-mRNA anchoring proteins (60). Sec61α, the primary ER ribosome receptor and protein conducting channel component (80,81) was highly enriched in the BrR fraction (Fig.5B). Similar to TRAPα, Sec61α was identified as a candidate HeLa RBP (60). Interestingly, Sec61β, a subunit of the Sec61 complex, was also identified as a HeLa RBP (60), suggestive of a candidate mRNA anchor function for the Sec61 complex. Intriguingly, all three proteins are members of hetero-oligomeric complexes and have established functions in post-translational protein modification, protein translocation, and/or ribosome binding, yet do not encode canonical RNA binding motifs (68,78,79,81,82). Emerin, an inner nuclear envelope protein integral membrane protein, was included as an additional control and was recovered uniquely in the BrR fraction.

In a parallel series of experiments, we performed a quantitative 'polysome-interactome' screen for proteins that associate with cytosolic, BrS-, and/or BrR-derived polysomes. Here, triplicate independent cell fractionation experiments were performed where polysomes from the cytosol, BrS and BrR fractions were purified using sucrose density gradient and their protein compositions analyzed by quantitative 2D-LC/MS/MS (Fig.5C-F, Table S2). In this experiment, we sought to selectively capture biochemically stable (e.g., resistant to high salt-, EDTA-, and/or Brij35 solubilization) mRNA-protein interactions characteristic of the endomembrane protein mRNAs (13,15). A modification of the absolute quantification 2D LC/MS/MS methods developed by Silva and Geromanos was used for protein quantification (40,41,83). In this method, samples are spiked with protein standards, with the mass

spectrometric signal response from the trypsin-generated, protein standard-derived peptides providing a signal response factor (counts/mol protein) that is then used to determine the concentrations of identified proteins.

The primary features of this data set are summarized in Fig.5C-E, with the complete data set included in Table S2. The MS analysis yielded the identification of 283 proteins identified at high confidence (> 2 peptides), with 3433 peptides providing spectral data for identification and quantification. The quantitative data represented in Fig. 5C are limited to those proteins which were identified and quantified in at least two of the three independent biological replicates. This additional selection reduced the number of proteins analyzed to 238. Polysome protein compositions of the three fractions were quite similar for the high abundance proteins comprised predominately of ribosomal proteins, but show significant compositional divergence for the lower-abundance proteins that include RBPs and ER membrane proteins. A hierarchical clustering analysis of these data is shown in Fig.5D and demonstrates the high similarities between the individual sample replicates as well as the subcellular variations in polysome composition, where the BrR-derived polysomes were the most divergent, and the cytosol- and BrS-derived polysomes the most similar. These data further highlight the distinct biochemical composition of the BrR ER-associated polysomes as detailed below.

To focus on polysome-interacting proteins enriched in the BrR, enrichment profiles were determined where we examined the relative partitioning of identified proteins in the total ER (BrR + BrS) polysomes vs. enrichment in the BrR polysomes (Fig.5E). Here we note that those proteins that are highly enriched on the ER are also highly enriched in the BrR polysome fraction (upper right quadrant, Fig.5E). Conversely, the BrS polysomes display proteins that are either not ER-enriched (lower left quadrant, Fig.5E) or are present in both BrS and BrR fractions. Thus, the BrR polysomes possess more proteins that are unique to the ER, whereas BrS polysomes are more accurately described as generic – they are representative of the median polysome protein composition and translate a large fraction of the transcriptome. Notably, the prominent protein cluster at 0.66 ER enrichment is predominately ribosomal proteins, which are largely common to both the ER-associated polysome fractions. In comparing the BrR and BrS polysomes, particularly striking differences were noted in the enrichments of ER membrane proteins, exon-junction complex (EJC) and nonsense-mediated decay (NMD) components (Fig.5F), and these findings are presented below.

In Fig.5F are listed selected categories of polysome-associated proteins and their relative subcellular distributions in the cytosolic- (C), BrS-, and BrR-derived polysomes. ER resident membrane proteins identified in this analysis (Sec61α, Sec61β, and ribophorin I) are members of the candidate ER-mRNA anchoring proteins proposed above and previously identified as members of the HeLa mRNA interactome or as candidate HeLa RBPs (60). In addition, the relative ER distributions identified in the Brij35 solubilization profile experiments (Fig.5B) were closely mirrored in the polysome-interactome analysis, with the two Sec61 subunits being uniquely recovered in the BrR-derived polysome fraction and ribophorin I being recovered in both the BrS- and BrR-derived polysome fractions. These data thus identify a subset of ER membrane proteins that are selectively bound, directly or indirectly, to the BrR-derived polysomes, and thus represent candidate selective ER mRNA anchoring proteins.

In the category '*General Polysome'* the fractional distributions of guanine nucleotide-binding protein β2 (RACK1), a prominent ribosome-associated protein, poly(A) binding protein 4 (PABP1), UPF1 (RENT1) and eIF6 were similar between the three polysome fractions, and serve as internal validation of the quantitative proteomic approach. For the category '*Cytosol Enriched*', we highlight two proteins, GAPDH, which was recently identified as an mRNA binding protein, and the nascent chain associated complex (NAC), which participates in protein folding and protein targeting to the ER. In the category '*ER-Enriched"* we identified the core exon junction complex component eIF4AIII as highly enriched on ER-associated polysomes. The remaining EJC core components Magoh, Y14, and Barentz were not identified. As this analysis is limited to polysome-recruited mRNAs, the absence of Magoh, Y14, and Barentz may reflect

the release of these factors upon translation and/or EJC remodeling, as previously reported (84,85). EJC interacting proteins with similar, ER-enriched subcellular distributions included Pinin and ACINU. That these proteins were identified on translationally active polysomes is suggestive of cytosolic functions complementary to their established roles in nonsense-mediated decay; such functions could include roles in mRNA localization and/or anchoring to the ER. The enrichment of EJC and splicing factors in the HeLa BrR-derived polysome fraction did, however, raise the concern of cross-contamination with nuclear-derived mRNA-splicing complexes. To determine if the BrR polysome fraction contained nuclear-derived splicing complexes, we screened for nuclear integrity/spliceosome release at each stage of the cell fractionation procedure. We found that the nuclear envelope integrity was disrupted at the Brij35 solubilization stage, yielding release of the nuclear proteins histone H3F3A, hnRNPA1, and HuR into the BrS fraction (data not shown) and indicating that passive contamination of the BrR fraction by nuclear components was unlikely. As well, Brij35 treatment yielded the release of U2 and U4 snRNAs, both of which were recovered in the slow migrating region of a velocity sedimentation experiment, separated from the polysome fraction (data not shown). These data provide additional support for the conclusion that the subset of EJC/NMD proteins co-purifying with the BrR polysomes are in fact polysome-associated. Whether or not they participate in mRNA anchoring to the ER is unknown; it is equally plausible that they are associated with newly exported mRNAs that undergo selective translation on ER-associated ribosomes. In summary, the results of the polysome-interactome screen support a model where the ER-mRNA transcriptome is comprised of populations of functionally-related mRNAs bearing distinct RBP 'fingerprints' and which are anchored to the ER by distinct mechanisms.

Of the candidate ER mRNA anchoring proteins identified in the polysome-interactome screen, both Sec61α and ribophorin I have been previously reported to function as ribosome receptors (81,86). Their identification in a polysome-interactor proteomic screen could, therefore, reflect ribosome- rather than mRNA-binding, function (81,86). For this reason, a third independent experimental approach was developed. Here, we again utilized canine pancreas RM as the source of ER-associated polysomes, reasoning that if the nuclear proteins identified in the HeLa polysome interactome screen were derived from cross-contamination, they would be largely absent from the ER-associated mRNPs. To address the question of mRNA versus rRNA binding activity, purified RM-derived polysomes were adjusted to 10 mM EDTA to dissociate the ribosomal subunits and their associated mRNAs (87) and the rRNA-free poly(A) mRNPs purified by native affinity chromatography on oligo-dT in the presence of 10 mM EDTA (Fig.8A). As an additional specificity control, identical quantities of ER-derived polysomes were digested with staphylococcal nuclease prior to oligo-dT chromatography and the nuclease-digested fraction processed in parallel. A proteomic analysis was then conducted on the fractions eluted in low salt/formamide buffers, elution conditions selective for mRNA release (Fig. 8B).

The protein composition of the RNPs purified by native oligo-dT chromatography was determined by mass spectrometry of in-gel digested gel fragments (1D SDS-PAGE/LC/MS/MS). These results are summarized in Fig.8B, with a full listing included in Table S3, and are limited to those proteins that were identified in at least two of three independent experiments, absent from the staphylococcal nuclease-treated controls, and whose identification was determined at high accuracy ($p < 0.05$, peptide count ≥ 2). In total, 170 proteins were identified, with 72 proteins meeting all criteria for selection.

As detailed in Table S3, 26 ribosomal proteins were identified, including proteins of the large and small ribosomal subunits. Of the 26 identified here, 18 were previously identified in the HeLa mRNA interactome and thus are likely to undergo direct interactions with poly(A) mRNAs (60). When compared to the HeLa polysome-interactome screen, this analysis yielded a substantially higher number of RNA binding proteins and translation factors, reflecting the additional proteomic depth achieved by analyzing ribosome-free mRNPs. As summarized in Fig.8B, nearly all proteins identified as native poly(A) mRNA interactors in the canine ER-associated mRNP screen were also identified in the recent HeLa mRNA interactome study of (60). That we

were able to identify this diversity of RBPs under native conditions demonstrates that these RBPs are stably bound to their target mRNAs.

The native mRNA interactome of the ER-associated poly(A) mRNA pool includes the EJC/NMD factors eIF4AIII and UPF1, further corroborating the identification of these proteins in the ER-associated HeLa polysomes and providing additional independent evidence that these proteins can stably associate with ribosome-engaged mRNAs. A substantial number of the snRNP/SR/hnRNP proteins identified in our HeLa polysome interactome screen and in the HeLa mRNA interactome were also identified as interactors in the canine RM-derived mRNP analysis, and so it can also be concluded that these proteins are present on translationally active, ER-associated polysomes and likely have functions extending beyond their roles in nonsense-mediated decay.

In a complementary series of experiments, RM were UV-irradiated to photocrosslink bound mRNAs to their interacting protein partners and the RM then solubilized in lithium SDS (Li-SDS). UV-crosslinked mRNA-protein complexes were purified by affinity chromatography on oligo-dT in the presence of 0.5M LiCl and Li-SDS and mRNA bound proteins selectively eluted by addition of RNaseA/T1. The composition of this fraction was interrogated by immunoblot analysis (Fig. 8C). Of primary interest is the identification of Sec61α, Sec61β, and ribophorin I as poly(A) mRNA-associated ER membrane proteins. Importantly, other ER membrane proteins identified as mRNA binding proteins in prior screens, such as CKAP4 and LRC59, were not detected in the nuclease eluate and thus may be mRNA-associated via indirect interactions. With respect to Sec61α, Sec61β, and ribophorin I, multiple, independent lines of experimental evidence now contribute to their identifications as mRNA binding proteins and include, in addition to the data reported above, UV and 4-thiouridine photocrosslinking, as reported in the HeLa mRNA interactome (60); selective enrichment on polysomes solubilized from the Brij-resistant ER of HeLa cells; and identification as native poly(A) mRNA binding proteins of canine pancreas RM-derived mRNPs (Fig.8B). In total, these data support a function for the Sec61 complex, subunits of the oligosaccharyltransferase complex, and to a lesser degree, the translocon-associated protein complex, in the direct anchoring of mRNAs to the ER. The identification of p180 in the RM, but not HeLa-derived fractions, is consistent with prior reports that p180 is highly expressed in terminally differentiated 'professional' secretory cells but only very weakly in HeLa cells, where it did not meet statistical criteria for selection in the mRNA interactome or as a candidate RNA binding protein (60,76). Thus, we are unable to identify a role for p180 in the direct anchoring of endomembrane protein-encoding mRNAs to the HeLa ER, though a related function in terminally differentiated secretory cells remains plausible.

Discussion:

Studies in diverse organisms have revealed an extensive functional interplay between the processes of mRNA localization, translation, and decay and the endoplasmic reticulum (ER) (19,88,89)). With recent genome-scale analyses demonstrating a broad representation of the mRNA transcriptome on the ER, there is now a pressing need to understand how mRNAs are selected, localized, and anchored to the ER. We address the latter question here, focusing on the mRNAs encoding the resident proteins of the endomembrane system, an essential gene family comprising over 500 genes and distinguished by a direct, ribosome-independent mode of membrane association (13,15). Here we provide evidence that subunits of the Sec61 and oligosaccharyltransferase complexes function as ER-mRNA anchoring proteins.

In microsomes, endomembrane protein-encoding mRNAs are distinguished from secretory protein-encoding mRNAs by their capacity to remain membrane associated following extraction of bound ribosomes with high salt and/or EDTA (13,15). This finding suggested a relatively simple biochemical distinction in the two ER-mRNA association mechanisms, where secretory protein-encoding mRNAs are anchored via their engagement on membrane bound ribosomes, and endomembrane protein-encoding mRNAs engage in direct binding interactions with components of the ER. In semi-intact HeLa cells, this distinction was recapitulated by sequential detergent fractionation with detergents (Brij-family) that

selectively solubilize the glycerolphospholipid but not sphingolipid fraction of biological membranes. Given the selective Brij-sensitivity of ER-mRNA interactions, we thought it plausible that candidate integral membrane mRNA anchoring proteins would also display heterogeneous distributions in the detergent induced ER membrane domains and in studies with a subset of ER resident membrane proteins this was confirmed. These observations, coupled with UV-photocrosslinking studies demonstrating a diverse population of integral membrane RNA-interacting proteins, suggested a model where mRNAs are selectively anchored via interactions with membrane proteins. Quantitative proteomic analysis of polyribsomes purified from the cytosol, the Brij-sensitive, and the Brij-resistant ER domains provided evidence for such a model - polysomes from the Brij-resistant HeLa ER were markedly enriched in mRNAs encoding resident ER, Golgi and lysosomal proteins and were uniquely associated with the core translocon components Sec61α/β. These data supports a model where the endomembrane resident protein-encoding mRNAs are selectively and directly anchored to resident proteins of the ER. In such a model, core translocon components would function as RNA organizing centers to enable a spatial organization of gene expression on the ER, a proposal consistent with the RNA operon model (90,91).

At first glance, a role for translocon components in selective mRNA anchoring to the ER seems unlikely, as it implies a selective function (mRNA anchoring) for proteins that perform a general function (protein translocation). However, the Sec61 and oligosaccharyl transferase complexes exist in different hetero-oligomeric states and are in stoichiometric excess to translocation sites (92,93). It is thus reasonable to consider that these essential proteins may be multifunctional, where particular oligomeric forms function in mRNA and/or ribosome binding to the ER and other forms serve as the protein translocation machinery.

A central question raised by these data is why direct RNA anchoring appears to be selective for the endomembrane protein-encoding mRNAs. In one view, a cohort-selective mRNA binding activity would provide a mechanism for coordinate biogenesis of the endomembrane system and/or 'biogenesis domains' dedicated to pre-organelle assembly, as has been proposed for peroxisome biogenesis (reviewed in (59). Such a model may be of particular relevance to the remarkable enrichment of lysosomal resident protein-encoding mRNAs in the Brij-resistant ER.

An additional question arising from this study concerns the mechanism of ribosome binding to the ER. Though a somewhat contentious question, there is general agreement that the Sec61 complex is the primary ER ribosome receptor (81,94-96). A key observation leading to this assignment was that in native membranes, ribosome binding to Sec61 is highly salt resistant (81). In the current study we found that a substantial fraction of ER-bound polysomes are released in the presence of 0.5M salt/Brij35, that these polysomes are enriched in mRNAs encoding cytosolic secretory cargo proteins, and in contrast to polysomes engaged in the translation of endomembrane protein-encoding mRNAs, the solubilized polysomes did not contain detectable quantities of Sec61 subunits. Such data imply that ribosomes, in an mRNA-dependent manner, might either bind to membrane receptors other then the Sec61 complex, or alternatively, the ribosome-Sec61 binding interaction might vary as a function of the mRNA undergoing translation. Regardless, these data suggest that further investigation into the mechanism and diversity of ribosome association with the ER is needed.

In summary, we demonstrate that the mRNA infrastructure of the ER is complex, with endomembrane protein-encoding mRNAs undergoing selective association with components of the translocon. The challenge ahead is to determine the molecular mechanism(s) that enable the selective association of the endomembrane resident protein mRNAs with their ER resident membrane protein-binding partners. Curiously, although none of the interacting ER membrane proteins that we identify display the canonical RNA binding motifs identified in soluble RNA binding proteins, they possess stretches of basic residues in cytosolic-facing loops that could have selective RNA binding activity.

Given the large number of mRNAs that utilize a direct ER association mechanism, and the established complexity of *cis*-encoded mRNA localization signals in even the best characterized mRNA localization examples (97), it seems unlikely that a common ER localization 'zip-code'

would serve to direct mRNA localization to the ER. Consistent with this view, ER localization information has been demonstrated to reside in the transmembrane domain-coding region of placental alkaline phosphatase, and in the case of the yeast membrane protein Pmp1, a repeating UG-rich motif in the 3' UTR (17,22). Regardless of the apparent complexity, progress towards the identification of the RNA binding motifs present in these candidate RNA anchoring proteins and the sequence/2-D structural motifs they recognize will help identify the molecular organization of the ER-mRNA infrastructure.

Acknowledgements:

The authors thank Harold Erickson for conducting rotary shadowing electron microscopy analyses and for enthusiastic interest. We are also grateful to Sam Johnson, Director of the Duke Light Microscopy Core facility, for his thoughtful guidance and advice, and the staff of the Duke Microarray core facility for assistance with the microarray studies. We thank Srinivas Ramachandran for helpful advice on the bioinformatic and statistical data analyses and Angeline S.L. Tay for critical reading of the manuscript. We thank Matthias Gromeier and Mariano Garcia-Blanco of Duke University for antisera to H3F3A and HnRNPA1, respectively, Riqiang Yan (Lerner Research Institute) for reticulon antisera, and Kiyoko Ogawa-Goto (Nippei Research Institute, Japan) for antisera to p180. Supported by a grant from the NIH (GM101533 to CVN) and a bridge-funding award from the Duke University School of Medicine (CVN). The DeltaVision system was purchased with funding from NIH/NCRR Shared Instrumentation Grant 1S10RR027528-0.

References:

1. Blobel, G. (2000) Protein targeting. *Biosci Rep* **20**, 303-344
2. Palade, G. (1975) Intracellular aspects of the process of protein synthesis. *Science* **189**, 347-358
3. Walter, P., and Johnson, A. E. (1994) Signal sequence recognition and protein targeting to the endoplasmic reticulum membrane. *Annu. Rev. Cell Biol.* **10**, 87-119
4. Suh, J., and Hutter, H. (2012) A survey of putative secreted and transmembrane proteins encoded in the C. elegans genome. *BMC Genomics* **13**, 333
5. Martin, K. C., and Ephrussi, A. (2009) mRNA localization: gene expression in the spatial dimension. *Cell* **136**, 719-730
6. Medioni, C., Mowry, K., and Besse, F. (2012) Principles and roles of mRNA localization in animal development. *Development* **139**, 3263-3276
7. Blobel, G., Walter, P., Chang, C. N., Goldman, B. M., Erickson, A. H., and Lingappa, V. R. (1979) Translocation of proteins across membranes: the signal hypothesis and beyond. *Symp Soc Exp Biol* **33**, 9-36
8. Zimmermann, R., Eyrisch, S., Ahmad, M., and Helms, V. (2011) Protein translocation across the ER membrane. *Biochim Biophys Acta* **1808**, 912-924
9. Diehn, M., Eisen, M. B., Botstein, D., and Brown, P. O. (2000) Large-scale identification of secreted and membrane-associated gene products using DNA microarrays. *Nat Genet* **25**, 58-62.
10. Lerner, R. S., Seiser, R. M., Zheng, T., Lager, P. J., Reedy, M. C., Keene, J. D., and Nicchitta, C. V. (2003) Partitioning and translation of mRNAs encoding soluble proteins on membrane-bound ribosomes. *Rna* **9**, 1123-1137
11. Nicchitta, C. V., Lerner, R. S., Stephens, S. B., Dodd, R. D., and Pyhtila, B. (2005) Pathways for compartmentalizing protein synthesis in eukaryotic cells: the template-partitioning model. *Biochem Cell Biol* **83**, 687-695
12. Reid, D. W., and Nicchitta, C. V. (2012) Primary Role for Endoplasmic Reticulum-bound Ribosomes in Cellular Translation Identified by Ribosome Profiling. *J Biol Chem* **287**, 5518-5527
13. Chen, Q., Jagannathan, S., Reid, D. W., Zheng, T., and Nicchitta, C. V. (2011) Hierarchical regulation of mRNA partitioning between the cytoplasm and the endoplasmic reticulum of mammalian cells. *Mol Biol Cell* **22**, 2646-2658
14. Cui, X. A., Zhang, H., and Palazzo, A. F. (2012) p180 promotes the ribosome-independent localization of a subset of mRNA to the endoplasmic reticulum. *PLoS Biol* **10**, e1001336
15. Pyhtila, B., Zheng, T., Lager, P. J., Keene, J. D., Reedy, M. C., and Nicchitta, C. V. (2008) Signal sequence- and translation-independent mRNA localization to the endoplasmic reticulum. *Rna* **14**, 445-453
16. Kraut-Cohen, J., Afanasieva, E., Haim-Vilmovsky, L., Slobodin, B., Yosef, I., Bibi, E., and Gerst, J. E. (2013) Translation- and SRP-independent mRNA targeting to the endoplasmic reticulum in the yeast Saccharomyces cerevisiae. *Mol Biol Cell* **24**, 3069-3084
17. Loya, A., Pnueli, L., Yosefzon, Y., Wexler, Y., Ziv-Ukelson, M., and Arava, Y. (2008) The 3'-UTR mediates the cellular localization of an mRNA encoding a short plasma membrane protein. *Rna* **14**, 1352-1365
18. Nevo-Dinur, K., Nussbaum-Shochat, A., Ben-Yehuda, S., and Amster-Choder, O. (2011) Translation-independent localization of mRNA in E. coli. *Science* **331**, 1081-1084
19. Kraut-Cohen, J., and Gerst, J. E. (2010) Addressing mRNAs to the ER: cis sequences act up! *Trends Biochem Sci* **35**, 459-469
20. Glisovic, T., Bachorik, J. L., Yong, J., and Dreyfuss, G. (2008) RNA-binding proteins and post-transcriptional gene regulation. *FEBS Lett* **582**, 1977-1986
21. Lunde, B. M., Moore, C., and Varani, G. (2007) RNA-binding proteins: modular design for efficient function. *Nat Rev Mol Cell Biol* **8**, 479-490

22. Cui, X. A., Zhang, Y., Hong, S. J., and Palazzo, A. F. (2013) Identification of a region within the placental alkaline phosphatase mRNA that mediates p180-dependent targeting to the Endoplasmic Reticulum. *J Biol Chem*
23. Bai, J. Z., Leung, E., Holloway, H., and Krissansen, G. W. (2008) Alternatively spliced forms of the P180 ribosome receptor differ in their ability to induce the proliferation of rough endoplasmic reticulum. *Cell biology international* **32**, 473-483
24. Ogawa-Goto, K., Irie, S., Omori, A., Miura, Y., Katano, H., Hasegawa, H., Kurata, T., Sata, T., and Arao, Y. (2002) An endoplasmic reticulum protein, p180, is highly expressed in human cytomegalovirus-permissive cells and interacts with the tegument protein encoded by UL48. *J Virol* **76**, 2350-2362
25. Ogawa-Goto, K., Tanaka, K., Ueno, T., Tanaka, K., Kurata, T., Sata, T., and Irie, S. (2007) p180 is involved in the interaction between the endoplasmic reticulum and microtubules through a novel microtubule-binding and bundling domain. *Mol Biol Cell* **18**, 3741-3751
26. Ueno, T., Kaneko, K., Sata, T., Hattori, S., and Ogawa-Goto, K. (2012) Regulation of polysome assembly on the endoplasmic reticulum by a coiled-coil protein, p180. *Nucleic Acids Res* **40**, 3006-3017
27. Ueno, T., Tanaka, K., Kaneko, K., Taga, Y., Sata, T., Irie, S., Hattori, S., and Ogawa-Goto, K. (2010) Enhancement of procollagen biosynthesis by p180 through augmented ribosome association on the endoplasmic reticulum in response to stimulated secretion. *J Biol Chem* **285**, 29941-29950
28. Jagannathan, S., Nwosu, C., and Nicchitta, C. V. (2011) Analyzing mRNA localization to the endoplasmic reticulum via cell fractionation. *Methods Mol Biol* **714**, 301-321
29. Stephens, S. B., and Nicchitta, C. V. (2007) In vitro and tissue culture methods for analysis of translation initiation on the endoplasmic reticulum. *Methods Enzymol* **431**, 47-60
30. Stephens, S. B., and Nicchitta, C. V. (2008) Divergent regulation of protein synthesis in the cytosol and endoplasmic reticulum compartments of mammalian cells. *Mol Biol Cell* **19**, 623-632
31. Milam, S. L., Osawa, M., and Erickson, H. P. (2012) Negative-stain electron microscopy of inside-out FtsZ rings reconstituted on artificial membrane tubules show ribbons of protofilaments. *Biophysical journal* **103**, 59-68
32. Chomczynski, P., and Sacchi, N. (2006) The single-step method of RNA isolation by acid guanidinium thiocyanate-phenol-chloroform extraction: twenty-something years on. *Nat Protoc* **1**, 581-585
33. Bordier, C. (1981) Phase separation of integral membrane proteins in Triton X-114 solution. *J Biol Chem* **256**, 1604-1607
34. Nicchitta, C. V., and Blobel, G. (1993) Lumenal proteins of the endoplasmic reticulum are required to complete protein translocation. *Cell* **73**, 989-998.
35. Gilar, M., Olivova, P., Daly, A. E., and Gebler, J. C. (2005) Orthogonality of separation in two-dimensional liquid chromatography. *Anal Chem* **77**, 6426-6434
36. Gilar, M., Olivova, P., Daly, A. E., and Gebler, J. C. (2005) Two-dimensional separation of peptides using RP-RP-HPLC system with different pH in first and second separation dimensions. *J Sep Sci* **28**, 1694-1703
37. Dowell, J. A., Frost, D. C., Zhang, J., and Li, L. (2008) Comparison of two-dimensional fractionation techniques for shotgun proteomics. *Anal Chem* **80**, 6715-6723
38. Keller, A., Nesvizhskii, A. I., Kolker, E., and Aebersold, R. (2002) Empirical statistical model to estimate the accuracy of peptide identifications made by MS/MS and database search. *Anal Chem* **74**, 5383-5392
39. Nesvizhskii, A. I., Keller, A., Kolker, E., and Aebersold, R. (2003) A statistical model for identifying proteins by tandem mass spectrometry. *Anal Chem* **75**, 4646-4658
40. Silva, J. C., Denny, R., Dorschel, C., Gorenstein, M. V., Li, G. Z., Richardson, K., Wall, D., and Geromanos, S. J. (2006) Simultaneous qualitative and quantitative analysis of the Escherichia coli proteome: a sweet tale. *Molecular & cellular proteomics : MCP* **5**, 589-607

41. Silva, J. C., Gorenstein, M. V., Li, G. Z., Vissers, J. P., and Geromanos, S. J. (2006) Absolute quantification of proteins by LCMSE: a virtue of parallel MS acquisition. *Molecular & cellular proteomics : MCP* **5**, 144-156
42. Saka, H. A., Thompson, J. W., Chen, Y. S., Kumar, Y., Dubois, L. G., Moseley, M. A., and Valdivia, R. H. (2011) Quantitative proteomics reveals metabolic and pathogenic properties of Chlamydia trachomatis developmental forms. *Mol Microbiol* **82**, 1185-1203
43. Wilm, M., Shevchenko, A., Houthaeve, T., Breit, S., Schweigerer, L., Fotsis, T., and Mann, M. (1996) Femtomole sequencing of proteins from polyacrylamide gels by nano-electrospray mass spectrometry. *Nature* **379**, 466-469
44. Rapoport, T. A., Wiedmann, M., Kurzchalia, T. V., and Hartmann, E. (1989) Signal recognition in protein translocation across the endoplasmic reticulum membrane. *Biochem Soc Trans* **17**, 325-328
45. Cardelli, J., Long, B., and Pitot, H. C. (1976) Direct association of messenger RNA labeled in the presence of fluoroorotate with membranes of the endoplasmic reticulum in rat liver. *J Cell Biol* **70**, 47-58
46. Kruppa, J., and Sabatini, D. D. (1977) Release of poly A(+) messenger RNA from rat liver rough microsomes upon disassembly of bound polysomes. *J Cell Biol* **74**, 414-427.
47. Lodish, H. F., and Froshauer, S. (1977) Binding of viral glycoprotein mRNA to endoplasmic reticulum membranes is disrupted by puromycin. *J Cell Biol* **74**, 358-364
48. Beckers, C. J., Keller, D. S., and Balch, W. E. (1987) Semi-intact cells permeable to macromolecules: use in reconstitution of protein transport from the endoplasmic reticulum to the Golgi complex. *Cell* **50**, 523-534
49. Stephens, S. B., Dodd, R. D., Lerner, R. S., Pyhtila, B. M., and Nicchitta, C. V. (2008) Analysis of mRNA partitioning between the cytosol and endoplasmic reticulum compartments of mammalian cells. *Methods Mol Biol* **419**, 197-214
50. Freidlin, P. J., and Patterson, R. J. (1980) Heparin releases monosomes and polysomes from rough endoplasmic reticulum. *Biochem Biophys Res Commun* **93**, 521-527
51. Lande, M. A., Adesnik, M., Sumida, M., Tashiro, Y., and Sabatini, D. D. (1975) Direct association of messenger RNA with microsomal membranes in human diploid fibroblasts. *J Cell Biol* **65**, 513-528.
52. Veis, A., Leibovich, S. J., Evans, J., and Kirk, T. Z. (1985) Supramolecular assemblies of mRNA direct the coordinated synthesis of type I procollagen chains. *Proc Natl Acad Sci U S A* **82**, 3693-3697
53. Gorlich, D., Prehn, S., Hartmann, E., Kalies, K. U., and Rapoport, T. A. (1992) A mammalian homolog of SEC61p and SECYp is associated with ribosomes and nascent polypeptides during translocation. *Cell* **71**, 489-503
54. Schuck, S., Honsho, M., Ekroos, K., Shevchenko, A., and Simons, K. (2003) Resistance of cell membranes to different detergents. *Proc Natl Acad Sci U S A* **100**, 5795-5800
55. Simons, K., and Toomre, D. (2000) Lipid rafts and signal transduction. *Nat Rev Mol Cell Biol* **1**, 31-39
56. Raj, A., van den Bogaard, P., Rifkin, S. A., van Oudenaarden, A., and Tyagi, S. (2008) Imaging individual mRNA molecules using multiple singly labeled probes. *Nat Methods* **5**, 877-879
57. Pagano, R. E., Martin, O. C., Kang, H. C., and Haugland, R. P. (1991) A novel fluorescent ceramide analogue for studying membrane traffic in animal cells: accumulation at the Golgi apparatus results in altered spectral properties of the sphingolipid precursor. *J Cell Biol* **113**, 1267-1279
58. Axelsson, M. A., and Warren, G. (2004) Rapid, endoplasmic reticulum-independent diffusion of the mitotic Golgi haze. *Mol Biol Cell* **15**, 1843-1852
59. Dimitrov, L., Lam, S. K., and Schekman, R. (2013) The role of the endoplasmic reticulum in peroxisome biogenesis. *Cold Spring Harb Perspect Biol* **5**, a013243

60. Castello, A., Fischer, B., Eichelbaum, K., Horos, R., Beckmann, B. M., Strein, C., Davey, N. E., Humphreys, D. T., Preiss, T., Steinmetz, L. M., Krijgsveld, J., and Hentze, M. W. (2012) Insights into RNA biology from an atlas of mammalian mRNA-binding proteins. *Cell* **149**, 1393-1406
61. Hogan, D. J., Riordan, D. P., Gerber, A. P., Herschlag, D., and Brown, P. O. (2008) Diverse RNA-binding proteins interact with functionally related sets of RNAs, suggesting an extensive regulatory system. *PLoS Biol* **6**, e255
62. Song, Y., Jiang, Y., Ying, W., Gong, Y., Yan, Y., Yang, D., Ma, J., Xue, X., Zhong, F., Wu, S., Hao, Y., Sun, A., Li, T., Sun, W., Wei, H., Zhu, Y., Qian, X., and He, F. (2010) Quantitative proteomic survey of endoplasmic reticulum in mouse liver. *J Proteome Res* **9**, 1195-1202
63. Tsvetanova, N. G., Klass, D. M., Salzman, J., and Brown, P. O. (2010) Proteome-wide search reveals unexpected RNA-binding proteins in Saccharomyces cerevisiae. *PloS one* **5**
64. Pashev, I. G., Dimitrov, S. I., and Angelov, D. (1991) Crosslinking proteins to nucleic acids by ultraviolet laser irradiation. *Trends Biochem Sci* **16**, 323-326
65. Walter, P., and Blobel, G. (1983) Preparation of microsomal membranes for cotranslational protein translocation. *Meth. Enzym.* **96**, 84-93
66. Kikuchi, Y., Hishinuma, F., and Sakaguchi, K. (1978) Addition of mononucleotides to oligoribonucleotide acceptors with T4 RNA ligase. *Proc Natl Acad Sci U S A* **75**, 1270-1273
67. Mathias, R. A., Chen, Y. S., Kapp, E. A., Greening, D. W., Mathivanan, S., and Simpson, R. J. (2011) Triton X-114 phase separation in the isolation and purification of mouse liver microsomal membrane proteins. *Methods* **54**, 396-406
68. Prinz, A., Behrens, C., Rapoport, T. A., Hartmann, E., and Kalies, K. U. (2000) Evolutionarily conserved binding of ribosomes to the translocation channel via the large ribosomal RNA. *Embo J* **19**, 1900-1906
69. Stalder, L., Heusermann, W., Sokol, L., Trojer, D., Wirz, J., Hean, J., Fritzsche, A., Aeschimann, F., Pfanzagl, V., Basselet, P., Weiler, J., Hintersteiner, M., Morrissey, D. V., and Meisner-Kober, N. C. (2013) The rough endoplasmatic reticulum is a central nucleation site of siRNA-mediated RNA silencing. *Embo J* **32**, 1115-1127
70. Trcek, T., Sato, H., Singer, R. H., and Maquat, L. E. (2013) Temporal and spatial characterization of nonsense-mediated mRNA decay. *Genes Dev* **27**, 541-551
71. Sidrauski, C., and Walter, P. (1997) The transmembrane kinase Ire1p is a site-specific endonuclease that initiates mRNA splicing in the unfolded protein response. *Cell* **90**, 1031-1039
72. Gilmore, R., Blobel, G., and Walter, P. (1982) Protein translocation across the endoplasmic reticulum. I. Detection in the microsomal membrane of a receptor for the signal recognition particle. *J Cell Biol* **95**, 461-469
73. Shibata, Y., Voss, C., Rist, J. M., Hu, J., Rapoport, T. A., Prinz, W. A., and Voeltz, G. K. (2008) The reticulon and DP1/Yop1p proteins form immobile oligomers in the tubular endoplasmic reticulum. *J Biol Chem* **283**, 18892-18904
74. Voeltz, G. K., Prinz, W. A., Shibata, Y., Rist, J. M., and Rapoport, T. A. (2006) A class of membrane proteins shaping the tubular endoplasmic reticulum. *Cell* **124**, 573-586
75. Savitz, A. J., and Meyer, D. (1990) Identification of a ribosome receptor in the rough endoplasmic reticulum. *Nature* **346**, 540-544
76. Langley, R., Leung, E., Morris, C., Berg, R., McDonald, M., Weaver, A., Parry, D. A., Ni, J., Su, J., Gentz, R., Spurr, N., and Krissansen, G. W. (1998) Identification of multiple forms of 180-kDa ribosome receptor in human cells. *DNA and cell biology* **17**, 449-460
77. Dejgaard, K., Theberge, J. F., Heath-Engel, H., Chevet, E., Tremblay, M. L., and Thomas, D. Y. (2010) Organization of the Sec61 translocon, studied by high resolution native electrophoresis. *J Proteome Res* **9**, 1763-1771
78. Hartmann, E., Gorlich, D., Kostka, S., Otto, A., Kraft, R., Knespel, S., Burger, E., Rapoport, T. A., and Prehn, S. (1993) A tetrameric complex of membrane proteins in the endoplasmic reticulum. *Eur. J. Biochem.* **214**, 375-381

79. Kelleher, D. J., Kreibich, G., and and Gilmore, R. (1992) Oligosaccharyltransferase activity is associated with a protein complex composed of ribophorins I and II and a 48 kD protein. *Cell* **69**, 55-65
80. Beckmann, R., Spahn, C. M., Eswar, N., Helmers, J., Penczek, P. A., Sali, A., Frank, J., and Blobel, G. (2001) Architecture of the protein-conducting channel associated with the translating 80S ribosome. *Cell* **107**, 361-372
81. Görlich, D., Prehn, S., Hartmann, E., Kalies, K.-U., and Rapoport, T. A. (1992) A mammalian homolog of Sec61p and SecYp is associated with ribosomes and nascent polypeptides during translocation. *Cell* **71**, 489-503.
82. Kelleher, D. J., and Gilmore, R. (2006) An evolving view of the eukaryotic oligosaccharyltransferase. *Glycobiology* **16**, 47R-62R
83. Silva, J. C., Denny, R., Dorschel, C. A., Gorenstein, M., Kass, I. J., Li, G. Z., McKenna, T., Nold, M. J., Richardson, K., Young, P., and Geromanos, S. (2005) Quantitative proteomic analysis by accurate mass retention time pairs. *Anal Chem* **77**, 2187-2200
84. Dostie, J., and Dreyfuss, G. (2002) Translation is required to remove Y14 from mRNAs in the cytoplasm. *Curr Biol* **12**, 1060-1067
85. Gehring, N. H., Lamprinaki, S., Kulozik, A. E., and Hentze, M. W. (2009) Disassembly of exon junction complexes by PYM. *Cell* **137**, 536-548
86. Kreibich, G., Ulrich, B. C., and Sabatini, D. D. (1978) Proteins of rough microsomal membranes related to ribosome binding. I. Identification of ribophorins I and II, membrane proteins characteristic of rough microsomes. *J. Cell Biol.* **77**, 464-487
87. Longuet, M., Auger-Buendia, M. A., and Tavitian, A. (1979) Studies on the distribution of ribosomal proteins in mammalian ribosomal subunits. *Biochimie* **61**, 1113-1123
88. Blower, M. D. (2013) Molecular insights into intracellular RNA localization. *International review of cell and molecular biology* **302**, 1-39
89. Weil, D., and Hollien, J. (2013) Cytoplasmic organelles on the road to mRNA decay. *Biochim Biophys Acta* **1829**, 725-731
90. Morris, A. R., Mukherjee, N., and Keene, J. D. (2010) Systematic analysis of posttranscriptional gene expression. *Wiley interdisciplinary reviews. Systems biology and medicine* **2**, 162-180
91. Keene, J. D. (2007) RNA regulons: coordination of post-transcriptional events. *Nat Rev Genet* **8**, 533-543
92. Guth, S., Volzing, C., Muller, A., Jung, M., and Zimmermann, R. (2004) Protein transport into canine pancreatic microsomes: a quantitative approach. *Eur J Biochem* **271**, 3200-3207
93. Kelleher, D. J., Karaoglu, D., Mandon, E. C., and Gilmore, R. (2003) Oligosaccharyltransferase isoforms that contain different catalytic STT3 subunits have distinct enzymatic properties. *Mol Cell* **12**, 101-111
94. Menetret, J. F., Neuhof, A., Morgan, D. G., Plath, K., Radermacher, M., Rapoport, T. A., and Akey, C. W. (2000) The structure of ribosome-channel complexes engaged in protein translocation. *Mol Cell* **6**, 1219-1232
95. Morgan, D. G., Menetret, J. F., Neuhof, A., Rapoport, T. A., and Akey, C. W. (2002) Structure of the mammalian ribosome-channel complex at 17A resolution. *J Mol Biol* **324**, 871-886
96. Voorhees, R. M., Fernandez, I. S., Scheres, S. H., and Hegde, R. S. (2014) Structure of the Mammalian Ribosome-Sec61 Complex to 3.4 A Resolution. *Cell* **157**, 1632-1643
97. Hamilton, R. S., and Davis, I. (2011) Identifying and searching for conserved RNA localisation signals. *Methods Mol Biol* **714**, 447-466

Figure Legends:

Figure 1. Endoplasmic reticulum-associated mRNAs are partitioned between detergent-resistant and detergent-sensitive membrane domains.

(**A**) Schematic of experimental design depicting a sequential detergent fractionation approach to the analysis of ER-ribosome/mRNA interactions.

(**B**) 0.5M Tris, Brij35, or admixtures of Tris and Brij35, Brij58, Triton X-100, or CHAPSO were screened for their capacity to solubilize mRNAs encoding GRP94 (GRP94; yellow) or β2-microglobulin (B2M; blue).

(**C**) The distributions of mRNAs encoding B2M, vascular endothelial growth factor A (VEGF-A) and thrombopoietin (THPO) (yellow bars), and the ER proteins GRP94, BiP and calreticulin (blue bars), in the Brij35-sensitive fraction of HeLa cells was determined by qRT-PCR. Data depicted in panel B are an average of three independent experiments and in Panel C, six independent experiments. Error bars represent *SEM*.

(**D**) Polysomes from the Tris/Brij-sensitive (BrS) and the Tris/Brij-resistant (BrR) fractions were analyzed by sucrose gradient velocity sedimentation in the absence and presence of EDTA.

(**E**) Translation activity of BrS and BrR polysomes; HeLa cells were labeled with [^{35}S]Met/Cys in the presence or absence of cycloheximide, fractionated as in (**D**) and the ribosome-associated polypeptides in the gradient fractions quantified by liquid scintillation counting of the TCA-precipitated proteins.

(**F,G**) The distributions of B2M (**F**) and GRP94 (**G**) mRNAs in BrS- and BrR-derived polysomes fractions in the absence (solid lines) or presence (dotted lines) of EDTA.

(**H,I**) Rotary shadowing electron microscopy images of polysomes derived from the BrS (**H**) and BrR (**I**) fractions. Bar = 100 nm.

Figure 2. Analysis of ER morphology and mRNA distributions in detergent-fractionated HeLa cells.

HeLa cell cultures were either untreated (Unfractionated), extracted with digitonin-supplemented cytosol buffer (Post-Digitonin), sequentially extracted with digitonin-supplemented cytosol buffer followed by Tris/Brij35 (Post-Brij), or the identical series followed by extraction with dodecylmaltoside-supplemented buffers (Post-DDM).

(**A**) HeLa cells were fixed directly (Unfractionated), or following sequential detergent extraction, and stained for B2M and GRP94 mRNAs. Z-stack images were acquired on a DeltaVision microscope and deconvolved, maximum-intensity projected micrographs are depicted. Inset = normalized quantification of RNA counts. Spot counting was performed using the Bitplane Imaris software and default threshold settings. The total number of mRNAs/cell was determined for 10-45 cells and mean +/- *SEM* values are depicted.

(**B**) Cells were biosynthetically labeled with ER tracker blue-white DPX and fractionated as described above.

(**C**) Cells were fractionated as described above and stained for the ER lumenal protein GRP94.

(D) Cell cultures were biosynthetically labeled with BODIPY FL C5-ceramide and fractionated as described above.

(**E**) Hela cell cultures were biosynthetically labeled with BODIPY FL C5-ceramide, followed by single molecule fluorescence imaging of GRP94 and B2M mRNAs as described above.

Figure 3. cDNA microarray analysis of mRNA partitioning to the Brij35-resistant fraction of HeLa ER.

(**A,B**) Mixture modeling of mRNA enrichments in the Brij-resistant fraction. In (**A**) the red line depicts a normal distribution; in (**B**) the red line depicts a tailed, two-component distribution.

(**C-D**) (**C**) Depicted are the relative distributions of the three primary cohorts of mRNAs, those encoding cytosolic proteins (Cytosolic), secretory pathway cargo proteins (Cargo) or endomembrane resident proteins (Endo); (**D**) Cumulative gene density (CGD) distributions of the data presented in (**C**). Shown are the three primary mRNA categories noted in (**A**) with the distributions of the six mRNAs analyzed in Fig. 1C denoted, demonstrating the concordance between the qRT-PCR and cDNA microarray data sets.

(**E**) CGD distributions of the components of the endomembrane resident gene category.
(**F**) CGD distribution of the mRNA cohort encoding soluble secretory (Cargo-Sec) and membrane proteins (Cargo-Mem).
(**G-J**) analyses of gene distribution in the Brij35-resistant fraction as a function of encoded signal sequence hydrophobicity (**G**), mRNA length (**H**), ribosome loading density (**I**) or enrichment on the ER (**J**). Pearson's correlation coefficients are included as insets for each analysis.

Figure 4. UV-crosslinking reveals RNA-binding endoplasmic reticulum membrane proteins.
(**A**) Schematic of experimental protocol for the identification of ER integral membrane RNA binding proteins.
(**B**) Images of SDS-PAGE/Coomassie Blue-stained gels depicting the membrane protein enrichments obtained by Triton X-114 or alkali extraction, with protein loadings as membrane equivalents (derived from identical quantities of RM) or protein equivalents (identical quantities of total protein).
(**C**) Immunoblot analysis of ER lumenal proteins (GRP94, BiP) and ER membrane proteins (ribophorin I (RPNI1), Sec61α, or TRAPα in the aqueous (AP) or detergent (DP) phases of the Triton X-114-extracted RM, or the soluble (S) and membrane protein (P) fractions of alkali-extracted RM.
(**D**) Labeling of UV-irradiated ER membrane protein fractions via the [^{32}P] pCp/T4 RNA ligase protocol is ligase-dependent (lane 2) and reveals RNA binding ER membrane proteins common to Triton X-114 (lane 3) and alkali-extracted (lane 4) RM.

Figure 5. Quantitative 'polysome interactor' screen reveals compartmentalized polysome-interacting protein distributions.
(**A**) Fractions were analyzed by immunoblot for the indicated candidate ER membrane RNA binding proteins.
(**B**) Schematic of experimental design of polysome interactor screen: HeLa cells were fractionated to yield cytosol, Bris-sensitive ER and Brij-resistant ER compartments. Polysome fractions were purified by sucrose gradient velocity sedimentation and the heavy polysome fractions selected for quantitative proteomic analysis.
(**C**) Protein abundance rank distribution plot demonstrating high similarities in the abundant proteins, and divergent compositions of lower abundance proteins in the cytosol, BrS and BrR polysome fractions.
(**D**) Heat map of compositional divergence of cytosol and ER-derived polysomes. The heat map illustrates the protein compositional similarities between the triplicate experimental datasets. The cytosol and Brij-sensitive ER fractions were most similar, the Brij-resistant ER fraction the most divergent.
(**E**) Contour map of protein enrichment on the ER as a function of enrichment in the BrR ER, illustrating that the BrR-resistant ER fraction is more uniquely representative of the ER.
(**F**) Tabulated data highlighting the primary features of the 'polysome-interactor' screen data. Included in the figure are paired immunoblot analyses of protein distribution for a subset of the quantified proteins. A full listing of all identified proteins and their quantitative fractional enrichments is provided as a supplementary table.

Figure 6. Proteomic analysis of ER polysome-derived mRNPs identifies ER-mRNA interacting proteins.
(**A**) Schematic illustration of experimental protocol. Rough microsomes were detergent solubilized, the polysome fraction isolated by sucrose gradient velocity sedimentation, treated with EDTA to release associated ribosomes, and the poly (A) mRNPs chromatographed on oligo-dT7 cellulose.
(**B**) partial listing of identified proteins at high confidence ($p \leq 0.05$), with paired comparisons to the HeLa mRNA Interactome database as well as the HeLa 'polysome interactor screen.'
(**C**) RM were subjected to UV photocrosslinking, the membranes solubilized in Li-SDS, and poly(A) mRNAs purified by oligo-dT chromatography in Li-SDS. RNA-bound proteins were eluted by nuclease digestion and the eluted fraction analyzed by immunoblot.

Table 1. Characteristics of proxy secretory and endomembrane protein-encoding mRNAs and their encoded proteins. Signal Properties: SS = signal sequence; TM = transmembrane domain; HS = hydrophobicity score (average hydrophobicity score of the signal peptide calculated using Kyte-Doolittle amino acid hydrophobicity scores).

				mRNA Properties (length in nt)			Signal Properties*		
Category	**Gene**	**Protein Product**	**Intracellular Location**	**5' UTR**	**CDS**	**3' UTR**	**SS**	**TM**	**HS**
	B2M	β-2-microglobulin	Secreted	60	360	567	Yes	No	1.581
	VEGFA	Vascular endothelial growth factor A	Secreted	498	1239	1940	Yes	No	0.585
Cargo	THPO	Thrombopoietin	Secreted	215	1062	528	Yes	No	1.5
	GRP94/ HSP90 B1	Heat shock protein 90kDa β	ER lumen	105	2412	263	Yes	No	1.327
	BiP/ HSPA5	Heat shock 70kDa protein 5	ER lumen	261	1965	1747	Yes	No	1.384
Endo	CALR	Calreticulin	ER lumen	80	1254	595	Yes	No	2.089

Table 2. Two-sample Kolmogorov-Smirnov (KS) test results for pairwise comparisons of mRNA cohorts, calculated using the R statistical package. The distance statistic (D) indicates the population deviation and the associated *p*-value the population deviation probability. Populations exhibiting significant differences are indicated in bold font.

Population 1	Population 2	Distance (D)	P-value
Cytosolic	**Cargo**	**0.5754**	**2.20E-16**
Cytosolic	**Endo**	**0.674**	**2.20E-16**
Cargo	**Endo**	**0.2824**	**2.20E-16**
Endo	ER	0.0856	5.79E-02
Endo	Golgi	0.0474	9.19E-01
Endo	**Lyso**	**0.3375**	**4.27E-07**
Cargo	Mem	0.0369	9.11E-02
Cargo	Sec	0.0905	3.05E-04

Figure 1, Jagannathan et al.

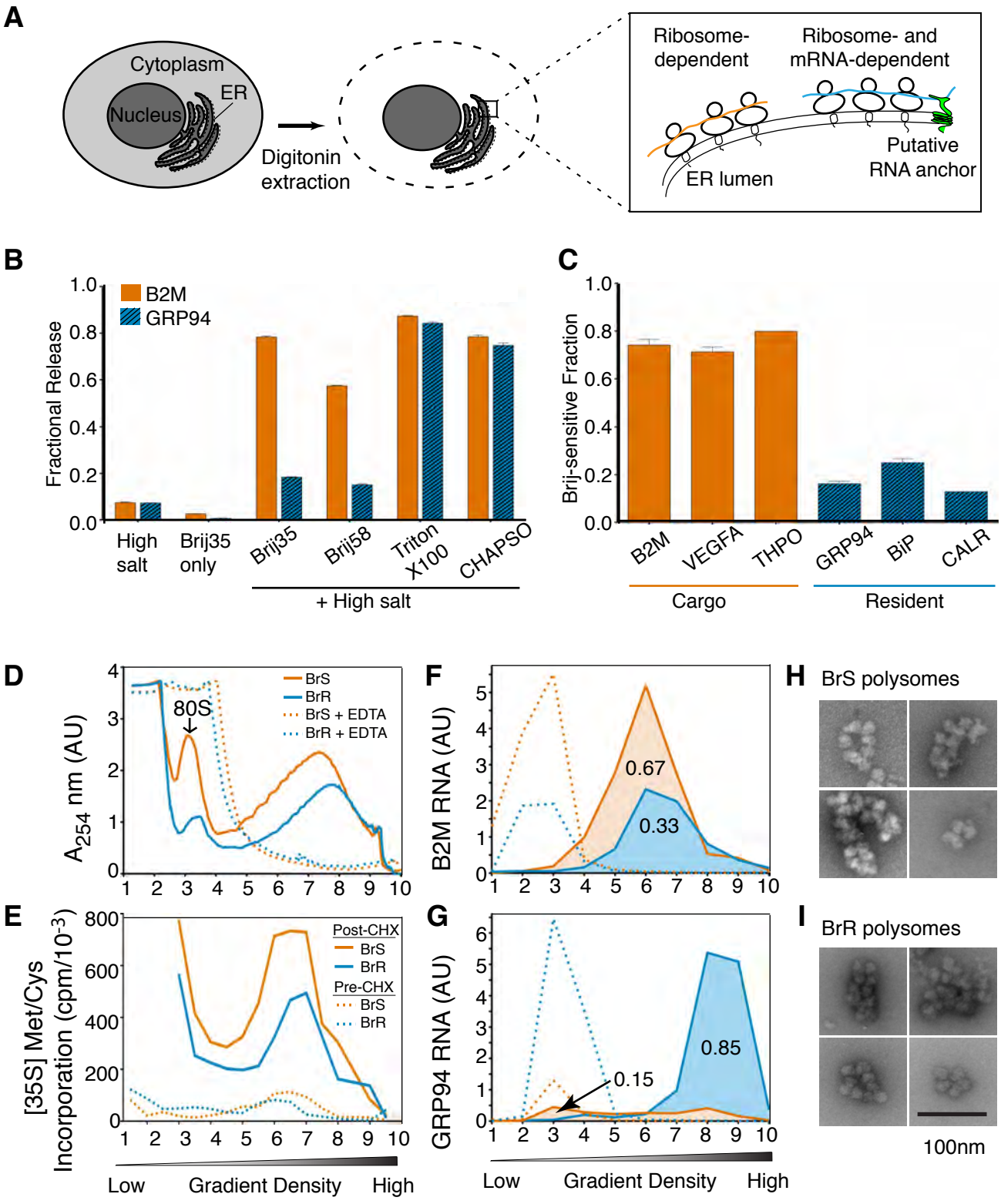

Figure 2, Jagannathan et al.

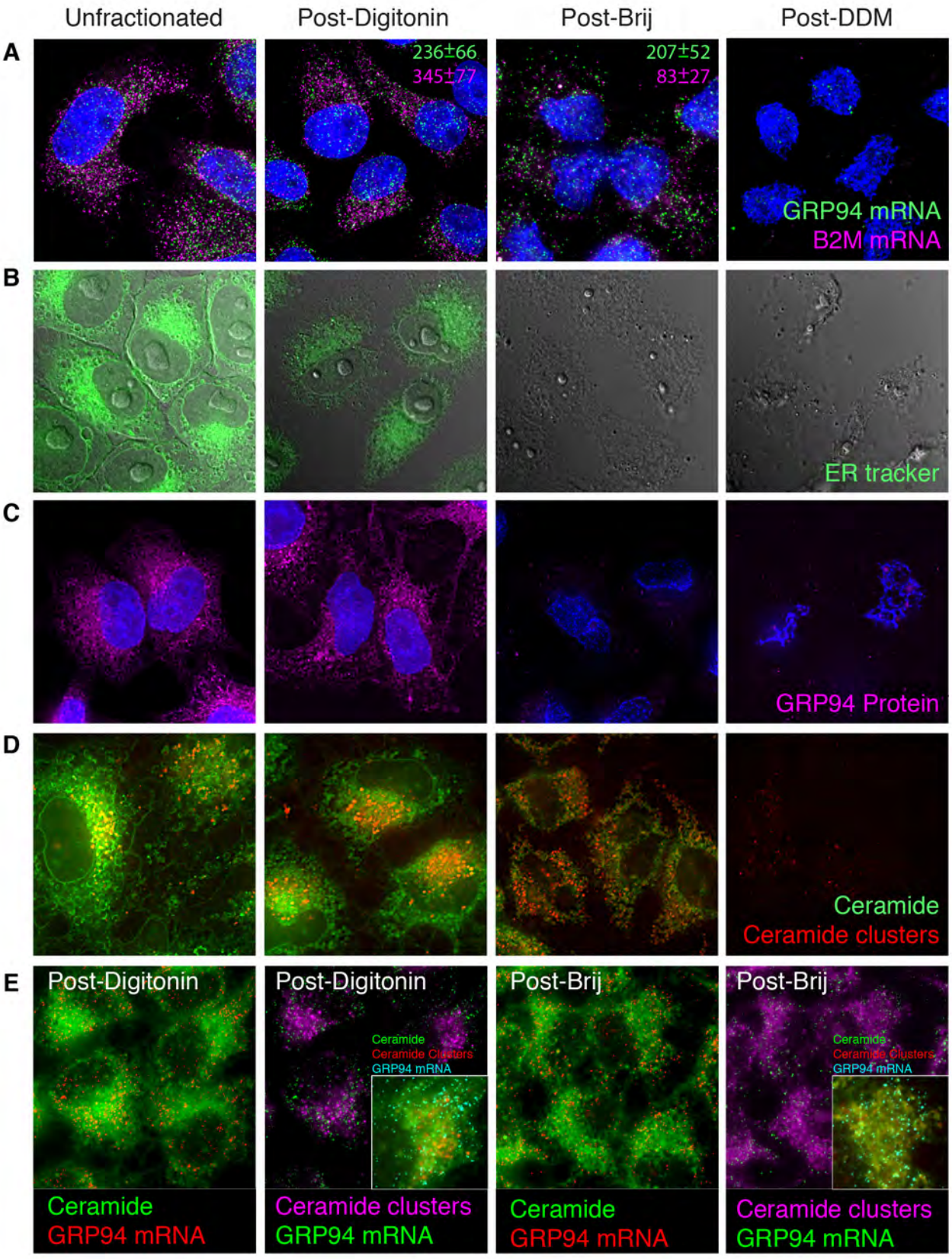

Figure 3, Jagannathan et al.

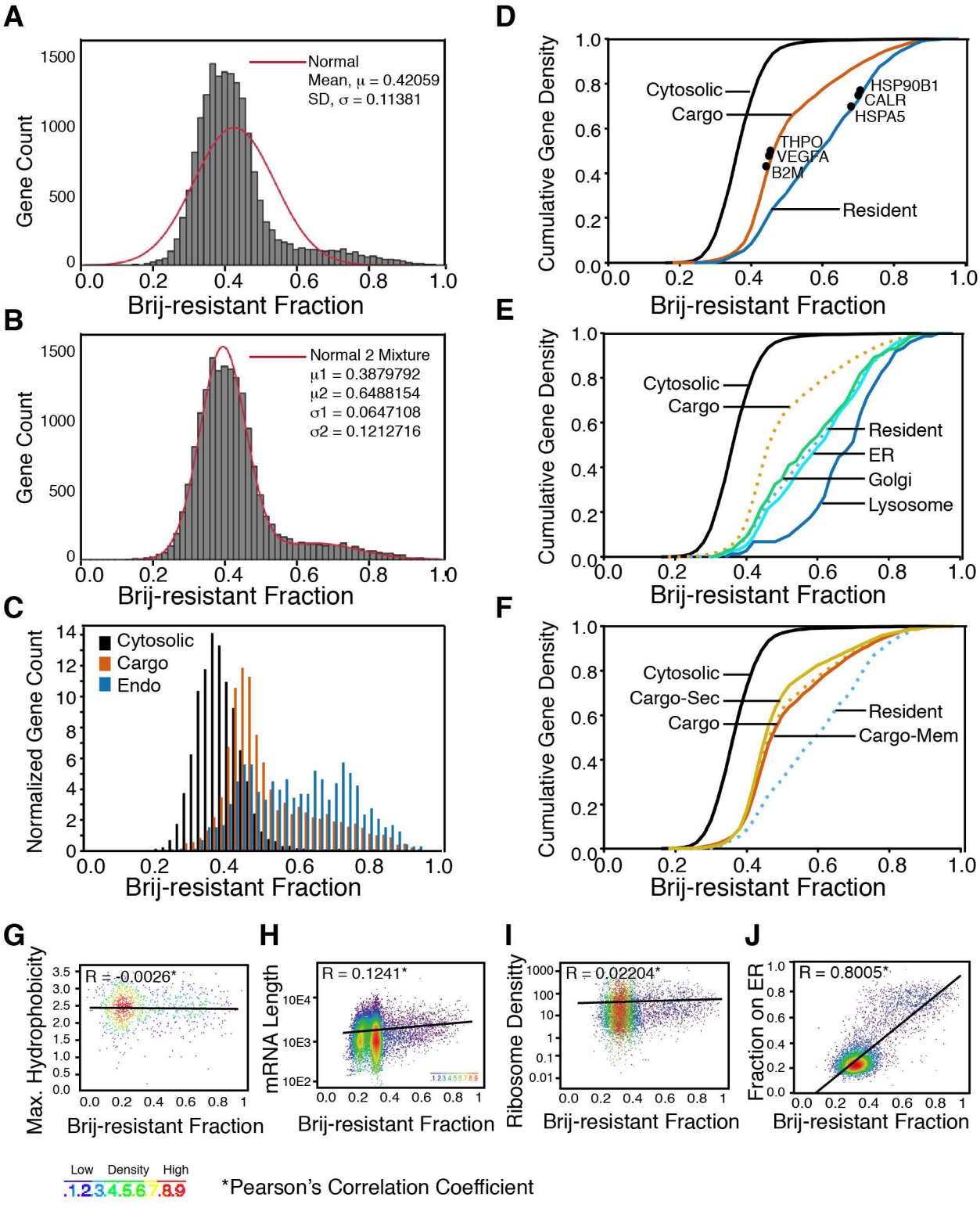

Figure 4, Jagannathan et al.

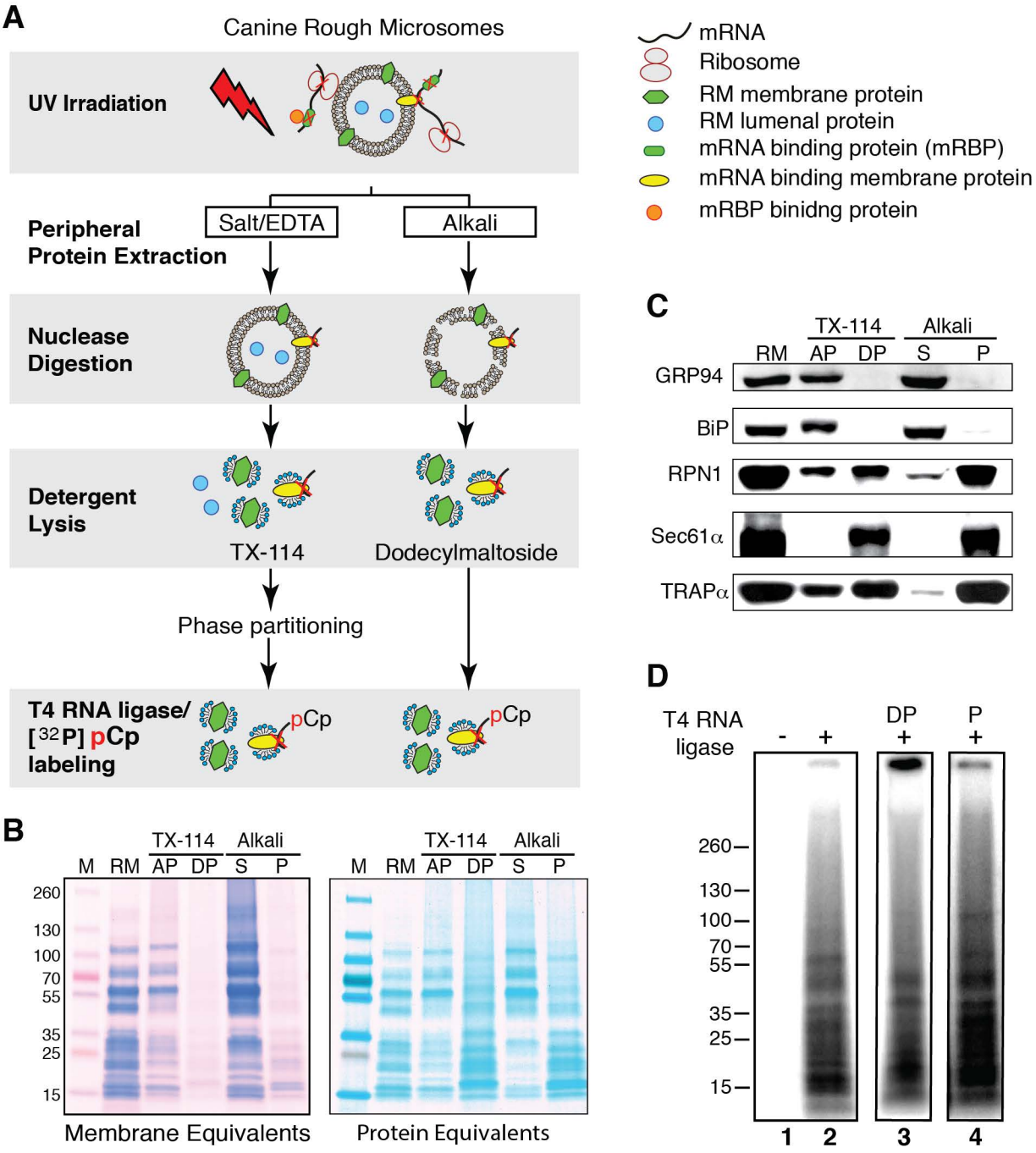

Figure 5, Jagannathan et al.

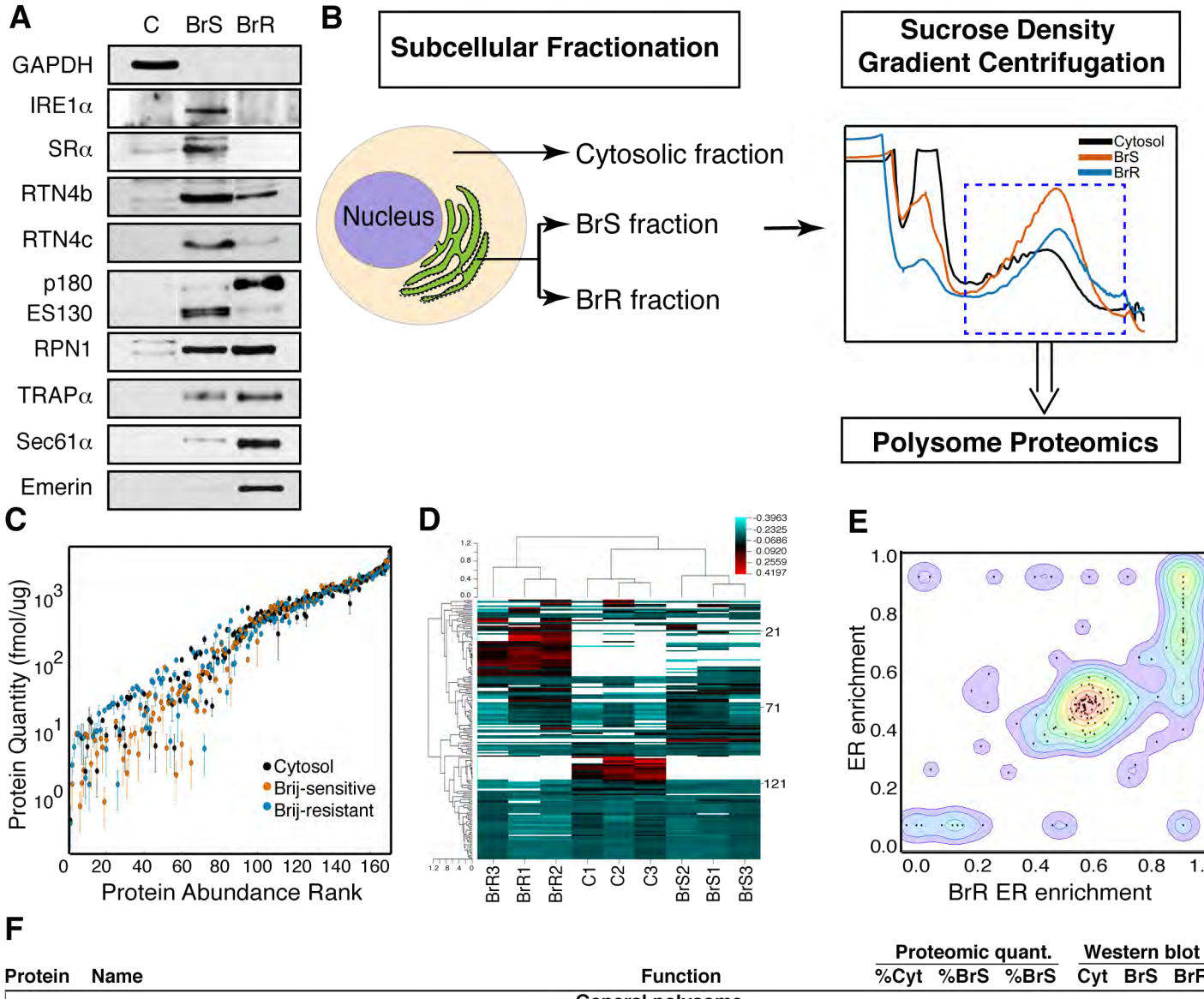

F

Protein	Name	Function	Proteomic quant. %Cyt	%BrS	%BrS	Western blot Cyt	BrS	BrR
		General polysome						
GBLP	Guanine nucleotide-binding protein beta-2	Signaling, translation regulation	36.8	32.4	30.8	ND		
PABP4	Polyadenylate-binding protein 4	Translation, mRNA binding	36.1	35.9	28.0			
RENT1	Regulator of nonsense transcripts 1	Nonsense mediated decay	24.8	38.1	37.1			
IF6	Eukaryotic translation initiation factor 6	80S assembly	25.1	34.8	40.1			
		Cytosol enriched						
G3P	Glyceraldehyde-3-phosphate dehydrogenase	Glycolysis, RNA binding	79.6	20.3	0.0			
NACA	Nascent polypeptide-associated complex subunit alpha	Suppress ER targeting	70.8	29.2	0.0	ND		
		ER enriched						
RPN1	Ribophorin 1	Glycosylation, ribosome binding	0.0	50.9	49.1	ND		
IF4A3	Eukaryotic initiation factor 4A-III	Exon junction complex	6.0	26.8	67.2			
PININ	Pinin	Exon junction complex	0.0	0.0	100.0	ND		
S61A1	Protein transport protein Sec61 subunit alpha	Protein translocation	0.0	0.0	100.0			
SC61B	Protein transport protein Sec61 subunit beta	Protein translocation	0.0	0.0	100.0			
GRP78	78 kDa glucose-regulated protein (BiP)	ER lumen chaperone	0.0	20.8	79.2			
CKAP4	Cytoskeleton-associated protein 4	ER microtubule anchoring	0.0	21.7	78.2	ND		

Figure 6, Jagannathan et al.

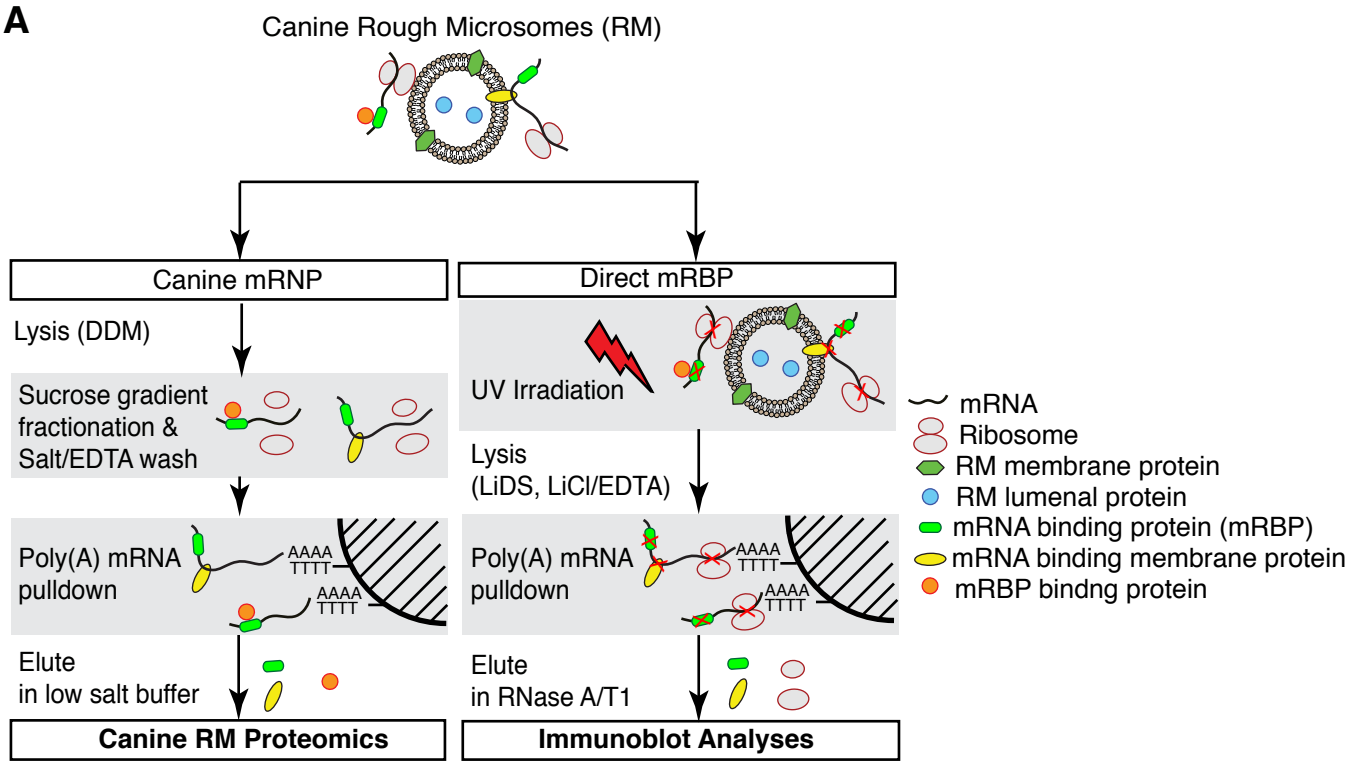

B

Canine mRNP	Name	Peptide count	HeLa mRNP (% in DDM)
RRBP1	Ribosome-binding protein 1 (p180)	88	ND
RPN2	Ribophorin 2	37	ND
MOGS	Mannosyl-oligosaccharide glucosidase	34	ND
SRPR	Signal recognition particle receptor subunit beta (SRβ)	34	ND
S61A1	Sec61 subunit alpha isoform 1(Sec61α)	20	100.0%
LRC59	Leucine-rich repeat-containing protein 59 (LRRC59)	20	ND
DGAT1	Diacylglycerol O-acyltransferase 1	18	ND
SRPRB	Signal recognition particle receptor subunit alpha (SRα)	17	ND
STT3A	Oligosaccharyl transferase subunit STT3A	15	ND
RPN1	Ribophorin 1	14	49.1%
LYRIC	Lysine-rich CEACAM1 co-isolated protein	14	ND
TRAM1	Translocating chain-associated membrane protein 1	11	ND
OST48	Oligosaccharyl transferase 48 kDa subunit	10	ND
PREB	Prolactin regulatory element-binding protein	10	ND
SSRA	Translocon-associated protein subunit alpha (TRAPα)	9	ND
PTSS1	Phosphatidylserine synthase 1	8	ND
ALG5	Dolichyl-phosphate beta-glucosyltransferase	6	ND
SPCS2	Signal peptidase complex subunit 2	6	ND
SC61B	Sec61 subunit beta (Sec61β)	5	100.0%
CKAP4	Cytoskeleton-associated protein 4 (Climp-63) (p63)	5	54.5%
SPCS3	Signal peptidase complex subunit 3	5	ND

C

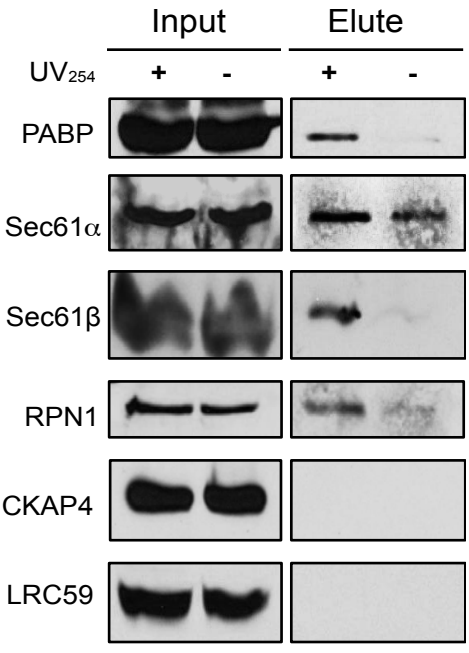

Multifunctional Roles for the Protein Translocation Machinery in RNA Anchoring to the Endoplasmic Reticulum

Sujatha Jagannathan, Jack C.-C. Hsu, David W. Reid, Qiang Chen, Will J. Thompson, Arthur M. Moseley and Christopher V. Nicchitta

J. Biol. Chem. published online July 25, 2014
